Behavior-type method for polarized Raman spectra of defects in cubic crystals

J. F. Zhou,* E. Goovaerts, and D. Schoemaker

Physics Department, University of Antwerp (Universitaire Instelling Antwerpen), B-2610 Wilrijk (Antwerp), Belgium
(Received 21 July 1983)

The intensity of polarized-light Raman scattering from a localized vibration of a point defect in a crystal is a discrete average over all the possible orientations of the defect. Much of the information contained in the Raman tensor of the vibrational mode is hidden by this discrete averaging. Partial or complete preferential reorientation or destruction of the defect, achieved by a so-called orientating operator $\hat{F}$, alters this average and permits in principle a determination of the symmetry of the defect, the nature of the modes, and the relative values of the elements of the Raman tensor. A discussion based on group theory is given for all of the possible symmetries of a point defect in a cubic lattice, as well as for all the possible symmetries of the orientating operator $\hat{F}$. The concept of *behavior type* of the Raman *intensity parameters* is introduced, which plays a central role in the application of the theory because it permits an efficient analysis of the data. The results are summarized in a series of tables. These are also helpful in choosing a suitable symmetry of the preferential orientating operator $\hat{F}$ (often from a polarized-light bleaching) and the suitable Raman polarization geometries. Similar methods can be applied to other host symmetries, and also to the study of the influence of an applied external field, e.g., an electric or stress field.

I. INTRODUCTION

Raman scattering has been widely used to study the properties of dynamical modes of point defects in crystals. The frequency shift of the scattered light yields the frequency of the dynamical mode. The Raman intensity depends on the polarization of the incident and scattered light[1,2] and permits, as will be discussed in this paper, determination to a large extent of the symmetry of the defect and the irreducible representation[3] to which the dynamical mode belongs.

The intensity of the Raman scattering from a localized dynamical mode of a point defect in a crystal is determined by the second-rank Raman tensor $\underline{T}$, the polarization vectors of the incident and scattered radiation, $\vec{a}$ and $\vec{b}$, respectively, and the intensity I_0 of the exciting light beam. The measured intensity I is further limited by the instrumental efficiency k:

$$I = kI_0(\vec{a}\,{}^t\underline{T}\vec{b})^2, \quad 0 \leq k \leq 1 . \tag{1}$$

The superscript t means "transpose." The dynamical mode is usually a localized vibration of the defect.

The observed intensity of a Raman line is the sum of the intensities from all the scattering defects. For a molecule which can freely take any orientation, e.g., in the gaseous state, the observed Raman scattering intensity is a continuous spatial average over all orientations in space. Thus only two independent parameters, namely, the mean polarizability α and the anisotropy γ can be obtained from Raman spectra. α and γ are composed of the elements of the Raman tensor.[1,2] A defect in a crystal can also occupy all its equivalent orientations which depend on the symmetry of both the host crystal and the defect. The resulting discrete space average in the crystal also obscures much of the information contained in the Raman tensor.

If the defects are equally distributed over all of their possible orientations in a crystal with cubic structure, three independent parameters (Sec. II B) can be obtained instead of the two parameters α and γ for scattering of freely rotating or of randomly orientated molecules.

The Raman scattering intensity of an isolated defect in a crystal is restricted by the symmetry and orientation of the defect and the nature of the dynamical mode. In this paper we will treat defects in crystals with the crystallographic point group O_h. The results are immediately applicable to the groups O and T_d and the treatment can be extended to other point groups. We will consider the defects to be initially randomly distributed over their possible orientations. A treatment is then applied which preferentially alters the populations of the different orientations. The most common of such treatments is a polarized optical bleaching in an absorption band of an anisotropic defect, but other methods can be applied. An orientating operator $\hat{F}$, acting on the populations, is used to describe this preferential orientation treatment. The symmetry of $\hat{F}$ is given by F'_1, the largest subgroup of the cubic point group O_h, which leaves the orientating operator $\hat{F}$ invariant.

The consequences of such a preferential orientation of the defects on the Raman scattering intensities will be theoretically investigated in Sec. II B. Every possible symmetry of the orientating operator $\hat{F}$ and of the defect, compatible with a cubic crystal structure, will be considered. The application of the theory to actual experiments will be discussed in Sec. III. The results are summarized in a series of tables which are useful in the analysis of experimental data. Final remarks about and a possible generalization of the present method will be given in Sec. IV.

We will adopt the following sets of reference axes in

this paper. The frame (x,y,z) is fixed to the principal crystal directions $\vec{x}||[100]$, $\vec{y}||[010]$, and $\vec{z}||[001]$, while the frame (x',y',z') is the local reference system for a defect with a given symmetry.

II. THEORY

A. Raman intensities for a general point defect in a cubic lattice

Consider a general defect in a crystal with a cubic-lattice structure. The defect has a certain orientation with respect to the surrounding crystal lattice. Performing all of the operations of the point group (Ref. 3) O_h on the defect, we find all its 48 possible orientations. We denote the nth orientation by v_n, the corresponding second-order Raman tensor by $\underline{T}^{(n)}$, and the set of orientations by V. By applying the rotations $\hat{R}_n \in O_h$ with rotation matrices $\underline{R}_n$ to an arbitrary original orientation v_1 of the defect, a homomorphic correspondence from the point group O_h to the set V is built up, in which the identity operator $\hat{E}$ corresponds to the orientation v_1 with Raman tensor $\underline{T}^{(1)}$ (see Table I and Fig. 1).

The rotations $\hat{R}_n \subset O$ are denoted by the symbols C_m^{α} (Table I) for clockwise rotation over $2\pi/m$ around an axis indicated by α. This axis is described in the (x,y,z) coordinate system, e.g., $\alpha = x\bar{y}$ stands for the $[1\bar{1}0]$ direction, while $\alpha = xy\bar{z}$ describes the $[11\bar{1}]$ crystalline direction.

A transformation operator $\hat{R}_n \in O_h$ acting on the crystal is equivalent to the inverse $\hat{R}_n^{-1}$ with rotation matrix $\underline{R}_n^t$, acting on the polarization vectors of the exciting and scattered light, if we consider the Raman scattering intensities:
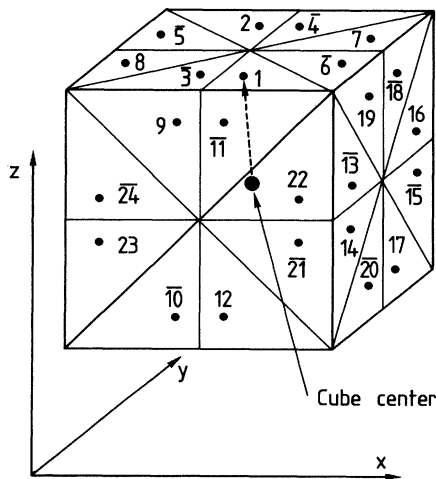

FIG. 1. Schematic representation of all possible orientations of a general point defect with symmetry $O_1 = C_1$ in a rocksalt structure, indicated by a vector. Only 24 of the 48 possible orientations are given in the figure; the others are at the back side. The numbers which indicate the orientations correspond to the numbers in Table I. The bars over the numbers in the figure mean that the corresponding rotations are improper ones.

$$I_n = kI_0[(\underline{R}_n^t\vec{a})^t\underline{T}^{(1)}(\underline{R}_n^t\vec{b})]^2$$
$$= kI_0(\vec{a}\,^t\underline{T}^{(n)}\vec{b})^2 , \tag{2a}$$

in which

$$\underline{T}^{(n)} = \underline{R}_n\underline{T}^{(1)}\underline{R}_n^t . \tag{2b}$$

As a trivial result one obtains that the Raman tensor is invariant under the inversion operator $\hat{i}$, which is equivalent to the identity $\hat{E}$ in calculating the Raman intensities. Thus from now on we shall reduce the size of the point groups by this equivalence and treat the orientations as being the same if they transform into each other under inversion. The homomorphic correspondence becomes that between the point group O and the set V which has 24 possible orientations for a general defect. Because the inversion transformation has no effect on the Raman tensor, the subgroups of O_h reduce to the subgroups of O. For example, C_{3v}, D_3, and D_{3d} reduce to D_3, and we call the subgroup $D_3 \subset O$ and its modes the representative of the subgroups $C_{3v},D_3,D_{3d} \subset O_h$ and their modes. This results in 11 subgroups of O and 40 modes as being the representatives of the 33 subgroups of O_h and the 124 modes (see Table II). From a subgroup $G \subset O$, but not the cubic point group itself or the tetrahedral point group $(G \neq O,T)$, one can obtain equivalent subgroups when the rotations $\hat{R} \in O$ are applied. For example, $D_4[100]$ can be rotated to $D_4[010]$ and $D_4[001]$. For the defect symmetry this rotation simply amounts to a different choice of the initial orientation v_1 and has no further consequences. For the representative symmetry $F_1 \subset O$ of the orientating operator $\hat{F}$ only one of these subgroups will be considered and listed in the tables. The results are in essence the same for the rotated subgroups, and when needed the rules will be given in order to adapt our results (see Sec. II D 2).

The observed Raman intensity I is the sum of the intensities I_n of the set of scattering orientations weighed by their population numbers N_n:

$$I = \sum_{n=1}^{24} N_n I_n , \tag{3}$$

with I_n given in (2a).

From Eqs. (2) and (3) one can write the observed Raman intensity as

$$I = kI_0 \sum_{n=1}^{24} N_n(\vec{a}\,^t\underline{T}^{(n)}\vec{b})^2$$
$$= kI_0 \sum_{i=1}^{3} \sum_{j=1}^{3} \sum_{i'=1}^{3} \sum_{j'=1}^{3} a_i b_j a_{i'} b_{j'} P_{iji'j'} , \tag{4}$$

with

$$P_{iji'j'} = \sum_{n=1}^{24} N_n T_{ij}^{(n)} T_{i'j'}^{(n)} . \tag{5}$$

There are 81 elements $P_{iji'j'}$, but because $\underline{T}^{(n)}$ is a symmetrical tensor, only 21 different $P_{iji'j'}$ are left. We call $P_{iji'j'}$ the Raman intensity parameter which we will denote from here on by IP. The 21 IP's contain all the information concerning the Raman tensor and the populations N_n which can be derived from the Raman scattering experiments.

TABLE I. Twenty-four Raman tensors are given corresponding to the 24 possible orientations of a defect with a general Raman tensor $\underline{T}^{(1)} \equiv \underline{T}$ in an arbitrary original orientation v_1. The tensors are classified according to the elements of the cubic group which is given as a direct product $O = D_2[100] \otimes D_3[111]$. The different orientations are given an identifying number for reference. Applying the rotation matrix on $\underline{T}^{(1)}$ [Eq. (2b)] yields the corresponding tensor $\underline{T}^{(n)}$. The defects are rotated with respect to the fixed reference system (x,y,z) (see Sec. II A).

	$D_3[111]$	$C_2^z D_3$	$C_2^z D_3$	$C_2^y D_3$
$D_2[100]$	1 $\ C_1 = \begin{pmatrix} 1 & & \\ & 1 & \\ & & 1 \end{pmatrix}$	2 $\ C_2^z = \begin{pmatrix} -1 & & \\ & -1 & \\ & & 1 \end{pmatrix}$	3 $\ C_2^z = \begin{pmatrix} 1 & & \\ & -1 & \\ & & -1 \end{pmatrix}$	4 $\ C_2^y = \begin{pmatrix} -1 & & \\ & 1 & \\ & & -1 \end{pmatrix}$
	$\begin{pmatrix} T_{11} & T_{12} & T_{13} \\ T_{21} & T_{22} & T_{23} \\ T_{31} & T_{32} & T_{33} \end{pmatrix}$	$\begin{pmatrix} T_{11} & T_{12} & -T_{13} \\ T_{21} & T_{22} & -T_{23} \\ -T_{31} & -T_{32} & T_{33} \end{pmatrix}$	$\begin{pmatrix} T_{11} & -T_{12} & -T_{13} \\ -T_{21} & T_{22} & T_{23} \\ -T_{31} & T_{32} & T_{33} \end{pmatrix}$	$\begin{pmatrix} T_{11} & -T_{12} & T_{13} \\ -T_{21} & T_{22} & -T_{23} \\ T_{31} & -T_{32} & T_{33} \end{pmatrix}$
$D_2 C_2^{\bar{x}y}$	5 $\ C_2^{\bar{x}y} = \begin{pmatrix} -1 & & \\ & -1 & \\ & & -1 \end{pmatrix}$	6 $\ C_2^{xy} = \begin{pmatrix} 1 & & \\ & 1 & \\ & & -1 \end{pmatrix}$	7 $\ C_4^x = \begin{pmatrix} -1 & & \\ & 1 & \\ & & 1 \end{pmatrix}$	8 $\ C_4^x = \begin{pmatrix} 1 & & \\ & -1 & \\ & & 1 \end{pmatrix}$
	$\begin{pmatrix} T_{22} & T_{21} & T_{23} \\ T_{12} & T_{11} & T_{13} \\ T_{32} & T_{31} & T_{33} \end{pmatrix}$	$\begin{pmatrix} T_{22} & T_{21} & -T_{23} \\ T_{12} & T_{11} & -T_{13} \\ -T_{32} & -T_{31} & T_{33} \end{pmatrix}$	$\begin{pmatrix} T_{22} & -T_{21} & -T_{23} \\ -T_{12} & T_{11} & T_{13} \\ -T_{32} & T_{31} & T_{33} \end{pmatrix}$	$\begin{pmatrix} T_{22} & -T_{21} & T_{23} \\ -T_{12} & T_{11} & -T_{13} \\ T_{32} & -T_{31} & T_{33} \end{pmatrix}$
$D_2 C_2^{\bar{y}z}$	9 $\ C_2^{\bar{y}z} = \begin{pmatrix} -1 & & \\ & -1 & \\ & & -1 \end{pmatrix}$	10 $\ C_4^z = \begin{pmatrix} 1 & & \\ & 1 & \\ & & -1 \end{pmatrix}$	11 $\ C_2^{yz} = \begin{pmatrix} -1 & & \\ & 1 & \\ & & 1 \end{pmatrix}$	12 $\ C_4^x = \begin{pmatrix} 1 & & \\ & -1 & \\ & & 1 \end{pmatrix}$
	$\begin{pmatrix} T_{11} & T_{13} & T_{12} \\ T_{31} & T_{33} & T_{32} \\ T_{21} & T_{23} & T_{22} \end{pmatrix}$	$\begin{pmatrix} T_{11} & T_{13} & -T_{12} \\ T_{31} & T_{33} & -T_{32} \\ -T_{21} & -T_{23} & T_{22} \end{pmatrix}$	$\begin{pmatrix} T_{11} & -T_{13} & -T_{12} \\ -T_{31} & T_{33} & T_{32} \\ -T_{21} & T_{23} & T_{22} \end{pmatrix}$	$\begin{pmatrix} T_{11} & -T_{13} & T_{12} \\ -T_{31} & T_{33} & -T_{32} \\ T_{21} & -T_{23} & T_{22} \end{pmatrix}$
$D_2 C_2^{\bar{z}x}$	13 $\ C_2^{\bar{z}x} = \begin{pmatrix} -1 & & \\ & -1 & \\ & & -1 \end{pmatrix}$	14 $\ C_4^y = \begin{pmatrix} 1 & & \\ & 1 & \\ & & -1 \end{pmatrix}$	15 $\ C_4^{\bar{y}} = \begin{pmatrix} -1 & & \\ & 1 & \\ & & 1 \end{pmatrix}$	16 $\ C_2^{zx} = \begin{pmatrix} 1 & & \\ & -1 & \\ & & 1 \end{pmatrix}$
	$\begin{pmatrix} T_{33} & T_{32} & T_{31} \\ T_{23} & T_{22} & T_{21} \\ T_{13} & T_{12} & T_{11} \end{pmatrix}$	$\begin{pmatrix} T_{33} & T_{32} & -T_{31} \\ T_{23} & T_{22} & -T_{21} \\ -T_{13} & -T_{12} & T_{11} \end{pmatrix}$	$\begin{pmatrix} T_{33} & -T_{32} & -T_{31} \\ -T_{23} & T_{22} & T_{21} \\ -T_{13} & T_{12} & T_{11} \end{pmatrix}$	$\begin{pmatrix} T_{33} & -T_{32} & T_{31} \\ -T_{23} & T_{22} & -T_{21} \\ T_{13} & -T_{12} & T_{11} \end{pmatrix}$
$D_2 C_3^{xyz}$	17 $\ C_3^{xyz} = \begin{pmatrix} 1 & & \\ & 1 & \\ & & 1 \end{pmatrix}$	18 $\ C_3^{x\bar{y}\bar{z}} = \begin{pmatrix} 1 & & \\ & -1 & \\ & & 1 \end{pmatrix}$	19 $\ C_3^{\bar{x}y\bar{z}} = \begin{pmatrix} 1 & & \\ & -1 & \\ & & -1 \end{pmatrix}$	20 $\ C_3^{\bar{x}\bar{y}z} = \begin{pmatrix} -1 & & \\ & 1 & \\ & & -1 \end{pmatrix}$
	$\begin{pmatrix} T_{33} & T_{31} & T_{32} \\ T_{13} & T_{11} & T_{12} \\ T_{23} & T_{21} & T_{22} \end{pmatrix}$	$\begin{pmatrix} T_{33} & T_{31} & -T_{32} \\ T_{13} & T_{11} & -T_{12} \\ -T_{23} & -T_{21} & T_{22} \end{pmatrix}$	$\begin{pmatrix} T_{33} & -T_{31} & -T_{32} \\ -T_{13} & T_{11} & T_{12} \\ -T_{23} & T_{21} & T_{22} \end{pmatrix}$	$\begin{pmatrix} T_{33} & -T_{31} & T_{32} \\ -T_{13} & T_{11} & -T_{12} \\ T_{23} & -T_{21} & T_{22} \end{pmatrix}$
$D_2 C_3^{\bar{x}\bar{y}z}$	21 $\ C_3^{\bar{x}\bar{y}z} = \begin{pmatrix} 1 & & \\ & 1 & \\ & & 1 \end{pmatrix}$	22 $\ C_3^{xy\bar{z}} = \begin{pmatrix} -1 & & \\ & -1 & \\ & & 1 \end{pmatrix}$	23 $\ C_3^{xyz} = \begin{pmatrix} 1 & & \\ & -1 & \\ & & -1 \end{pmatrix}$	24 $\ C_3^{\bar{x}yz} = \begin{pmatrix} -1 & & \\ & 1 & \\ & & -1 \end{pmatrix}$
	$\begin{pmatrix} T_{22} & T_{23} & T_{21} \\ T_{32} & T_{33} & T_{31} \\ T_{12} & T_{13} & T_{11} \end{pmatrix}$	$\begin{pmatrix} T_{22} & T_{23} & -T_{21} \\ T_{32} & T_{33} & -T_{31} \\ -T_{12} & -T_{13} & T_{11} \end{pmatrix}$	$\begin{pmatrix} T_{22} & -T_{23} & -T_{21} \\ -T_{32} & T_{33} & T_{31} \\ -T_{12} & T_{13} & T_{11} \end{pmatrix}$	$\begin{pmatrix} T_{22} & -T_{23} & T_{21} \\ -T_{32} & T_{33} & -T_{31} \\ T_{12} & -T_{13} & T_{11} \end{pmatrix}$

TABLE II. Subgroups $F'_1 \subset O_h$ which are considered for the orientating operator $\hat{F}$ are classified into sets indicated by their 11 representative symmetries $F_1 \subset O$, relevant in Raman scattering. Also listed are σ, the number of independent population numbers N_n, and μ_{IP}, the number of independent Raman IP's.

F_1	σ	μ_{IP}	F'_1
C_1	24	21	C_1, S_2
$C_2[100]$	12	13	$C_2[100], C_{1h}[100], C_{2h}[100]$
$C_2[011]$	12	13	$C_2[011], C_{1h}[011], C_{2h}[011]$
$D_2[100]$	6	9	$D_2[100,010,001], C_{2v}[100](010,001), D_{2h}\,[100,010,001]$
$D_2[011]$	6	9	$D_2[100,011,0\bar{1}1], C_{2v}[100](011,0\bar{1}1), C_{2v}[011](100,0\bar{1}1), D_{2h}[100,011,0\bar{1}1]$
$C_3[111]$	8	7	$C_3[111], S_6[111]$
$D_3[111]$	4	6	$D_3[111](1\bar{1}0,10\bar{1},01\bar{1}), C_{3v}[111](1\bar{1}0,10\bar{1},01\bar{1}), D_{3d}[111](1\bar{1}0,10\bar{1},01\bar{1})$
$C_4[100]$	6	7	$C_4[100], S_4[100], C_{4h}[100]$
$D_4[100]$	3	6	$D_4[100], C_{4v}[100], D_{4h}[100], D_{2d}[100,010,001](011,0\bar{1}1), D_{2d}[100,011,0\bar{1}1](010,001)$
T	2	3	T, T_h
O	1	3	O, T_d, O_h

Every matrix $\underline{R}_n \in O$ has the property that there is one element equal to 1 or -1 and two elements equal to 0 in each row and each column (see Table I), so that for each corresponding $\underline{T}^{(n)}$:

$$| T_{ij}^{(n)} | = | (\underline{R}_n \underline{T}^{(1)} \underline{R}_n^t)_{ij} | = | T_{i'j'}^{(1)} | \ , \tag{6}$$

in which the rotation $\hat{R}_n$ relates (i,j) to (i',j').

Performing 21 suitable measurements one obtains from Eq. (5) a set of linear equations:

$$I_1 = kI_0 \sum_{i=1}^{3} \sum_{j=1}^{3} \sum_{i'=1}^{3} \sum_{j'=1}^{3} a_{i,1} b_{j,1} a_{i',1} b_{j',1} P_{iji'j'} \ ,$$

$$I_2 = kI_0 \sum_{i=1}^{3} \sum_{j=1}^{3} \sum_{i'=1}^{3} \sum_{j'=1}^{3} a_{i,2} b_{j,2} a_{i',2} b_{j',2} P_{iji'j'} \ , \tag{7}$$

$$I_{21} = kI_0 \sum_{i=1}^{3} \sum_{j=1}^{3} \sum_{i'=1}^{3} \sum_{j'=1}^{3} a_{i,21} b_{j,21} a_{i',21} b_{j',21} P_{iji'j'} \ .$$

One can solve this set of linear equations for the IP if the polarization vectors $\vec{a}$ and $\vec{b}$ are suitably chosen. However, in most practical cases this is impossible, because the choice of the polarization vectors is often limited by the experimental setup, and because too many measurements with a high precision would be required. This problem will be discussed further in Secs. III B and III C. In most circumstances the constant k is unknown and as a result one can only obtain the relative IP values. For simplicity of notation, the 21 IP values will be denoted from here on by

$$q_1 = kI_0 P_{1111}, \quad q_2 = kI_0 P_{2222}, \quad q_3 = kI_0 P_{3333} \ ,$$

$$r_1 = kI_0 P_{2233}, \quad r_2 = kI_0 P_{1133}, \quad r_3 = kI_0 P_{1122} \ ,$$

$$s_1 = kI_0 P_{2323}, \quad s_2 = kI_0 P_{1313}, \quad s_3 = kI_0 P_{1212} \ ,$$

$$t_1 = kI_0 P_{1213}, \quad t_2 = kI_0 P_{1223}, \quad t_3 = kI_0 P_{1323} \ , \tag{8}$$

$$u_1 = kI_0 P_{1123}, \quad u_2 = kI_0 P_{2213}, \quad u_3 = kI_0 P_{3312} \ ,$$

$$v_1 = kI_0 P_{2223}, \quad v_2 = kI_0 P_{3323}, \quad v_3 = kI_0 P_{1113} \ ,$$

$$v_4 = kI_0 P_{3313}, \quad v_5 = kI_0 P_{1112}, \quad v_6 = kI_0 P_{2212} \ .$$

These IP values, which are the experimentally determined parameters, are the solutions of Eqs. (7) and, using Eq. (5), they are related to the population numbers and the Raman-tensor elements:

$$q_1 = kI_0 \sum_{n=1}^{24} N_n T_{11}^{(n)} T_{11}^{(n)} \ ,$$

$$q_2 = kI_0 \sum_{n=1}^{24} N_n T_{22}^{(n)} T_{22}^{(n)} \ , \tag{9}$$

$$v_6 = kI_0 \sum_{n=1}^{24} N_n T_{22}^{(n)} T_{12}^{(n)} \ .$$

The Raman tensors $\underline{T}^{(n)}$ are related to each other by Eq. (2b) (explicit expressions are given in Table I) and it is a long but straightforward calculation to determine the IP as a function of the population numbers N_n and the elements of only one Raman tensor, $\underline{T}^{(1)}$, corresponding to the initial orientation v_1 of the defect. These explicit expressions of the IP are given in Table III.

It is easy to see from Table III(a) that the IP $q_i \geq 0$ and $s_i \geq 0$, but the others can be either positive or negative. Similar to the IP, only the relative values of the N_n and the T_{ij} can possibly be determined in Raman experiments.

The Raman tensor, being a symmetrical second-rank tensor, possesses only six independent elements T_{ij}. There are 20 independent equations in (9) but up to 28 unknowns (5 T_{ij} and 23 N_n), taking into account that only relative values can be determined. Thus it is, in general, impossible to solve Eqs. (9) given an experimental set of IP's. In Sec. II B we shall see that after producing an anisotropy in the distribution of the orientation of the defects and after performing a sufficient number of experiments, it is in principle possible to solve Eqs. (9). But even so, because they are cubic equations, this is rather difficult and a high precision of the experimental data is required. Fortunately, a two-step approach to the solution of these equations is possible, as will be discussed in Sec. II D.

However, in many cases it is already of great value to identify the symmetry of the defect and the irreducible representations of its modes. To reach this more modest aim, it is in most cases not necessary to solve Eqs. (9) (see Sec. II D). As a result the analysis is feasible, since fewer experimental data with a lower precision are sufficient and the processing of the data is facilitated. In fact, once the symmetry of the defect and the irreducible representation of the mode are identified by the IP analysis, the number of independent T_{ij} and population numbers N_n, as well as the number of the independent IP's, are in most cases reduced by symmetry arguments, and Eqs. (9) become easier to solve. In some cases it remains impossible because not enough independent IP values are left.

B. Effect of the symmetry of the partial preferential orientation on the Raman intensities

Initially the populations N_n are all equal to each other, i.e., the defects are randomly distributed over all the possible equivalent orientations. As mentioned above a preferential orientation treatment, described by a so-called orientating operator $\hat{F}$, is applied to the defects. The symmetry of the orientating operator $\hat{F}$ is defined by the largest subgroup F_1 of O which leaves $\hat{F}$ invariant. The right cosets of F_1 will be indicated by [see Table IV(a)]

$$F_1, F_2, \ldots, F_\sigma \ .$$

There exists a homomorphic correspondence from the point group O to the orientation set V. The corresponding subsets of V are

$$V_1, V_2, \ldots, V_\sigma \ .$$

One can demonstrate (Appendix A) that after the orientating action of the operator $\hat{F}$ the populations N_n are equal if the orientations belong to the same subset V_r, i.e., if

$$v_p, v_q \in V_r, \quad r = 1, 2, \ldots, \sigma \tag{10a}$$

then

$$N_p = N_q \equiv \mathcal{N}_r \ . \tag{10b}$$

TABLE III. (a) Explicit expressions of the Raman IP's as defined in Eqs. (5) and (8) as a function of the Raman-tensor components T_{ij} of the dynamical mode in the original orientation v_1 and the parameters M. The latter are linear combinations of the population numbers N_n and are listed in (b).

(a)

$$q_1 = kI_0[(M_1 + M_3)T_{11}^2 + (M_2 + M_6)T_{22}^2 + (M_4 + M_5)T_{33}^2]$$
$$q_2 = kI_0[(M_2 + M_5)T_{11}^2 + (M_1 + M_4)T_{22}^2 + (M_3 + M_6)T_{33}^2]$$
$$q_3 = kI_0[(M_4 + M_6)T_{11}^2 + (M_3 + M_5)T_{22}^2 + (M_1 + M_2)T_{33}^2]$$

$$r_1 = kI_0[(M_1 + M_3)T_{22}T_{33} + (M_2 + M_6)T_{11}T_{33} + (M_4 + M_5)T_{11}T_{22}]$$
$$r_2 = kI_0[(M_2 + M_5)T_{22}T_{33} + (M_1 + M_4)T_{11}T_{33} + (M_3 + M_6)T_{11}T_{22}]$$
$$r_3 = kI_0[(M_4 + M_6)T_{22}T_{33} + (M_3 + M_5)T_{11}T_{33} + (M_1 + M_2)T_{11}T_{22}]$$

$$s_1 = kI_0[(M_1 + M_3)T_{23}^2 + (M_2 + M_6)T_{13}^2 + (M_4 + M_5)T_{12}^2]$$
$$s_2 = kI_0[(M_2 + M_5)T_{23}^2 + (M_1 + M_4)T_{13}^2 + (M_3 + M_6)T_{12}^2]$$
$$s_3 = kI_0[(M_4 + M_6)T_{23}^2 + (M_3 + M_5)T_{13}^2 + (M_1 + M_2)T_{12}^2]$$

$$t_1 = kI_0[(M_1' + M_3')T_{13}T_{12} + (M_2' + M_6')T_{23}T_{12} + (M_4' + M_5')T_{23}T_{13}]$$
$$t_2 = kI_0[(M_2'' + M_5'')T_{13}T_{12} + (M_1'' + M_4'')T_{23}T_{12} + (M_3'' + M_6'')T_{23}T_{13}]$$
$$t_3 = kI_0[(M_4''' + M_6''')T_{13}T_{12} + (M_3''' + M_5''')T_{23}T_{12} + (M_1''' + M_2''')T_{23}T_{13}]$$

$$u_1 = kI_0[(M_1' + M_3')T_{11}T_{23} + (M_2' + M_6')T_{22}T_{13} + (M_4' + M_5')T_{33}T_{12}]$$
$$u_2 = kI_0[(M_2'' + M_5'')T_{11}T_{23} + (M_1'' + M_4'')T_{22}T_{13} + (M_3'' + M_6'')T_{33}T_{12}]$$
$$u_3 = kI_0[(M_4''' + M_6''')T_{11}T_{23} + (M_3''' + M_5''')T_{22}T_{13} + (M_1''' + M_2''')T_{33}T_{12}]$$

$$v_1 = kI_0[M_1'T_{22}T_{23} + M_3'T_{33}T_{23} + M_2'T_{11}T_{13} + M_6'T_{33}T_{13} + M_4'T_{22}T_{12} + M_5'T_{11}T_{12}]$$
$$v_2 = kI_0[M_1'T_{33}T_{23} + M_3'T_{22}T_{23} + M_2'T_{33}T_{13} + M_6'T_{11}T_{13} + M_4'T_{11}T_{12} + M_5'T_{22}T_{12}]$$
$$v_3 = kI_0[M_2''T_{22}T_{23} + M_5''T_{33}T_{23} + M_1''T_{11}T_{13} + M_4''T_{33}T_{13} + M_3''T_{11}T_{12} + M_6''T_{22}T_{12}]$$
$$v_4 = kI_0[M_2''T_{33}T_{23} + M_5''T_{22}T_{23} + M_1''T_{33}T_{13} + M_4''T_{11}T_{13} + M_3''T_{22}T_{12} + M_6''T_{11}T_{12}]$$
$$v_5 = kI_0[M_4'''T_{33}T_{23} + M_6'''T_{22}T_{23} + M_3'''T_{11}T_{13} + M_5'''T_{33}T_{13} + M_1'''T_{11}T_{12} + M_2'''T_{22}T_{12}]$$
$$v_6 = kI_0[M_4'''T_{22}T_{23} + M_6'''T_{33}T_{23} + M_3'''T_{33}T_{13} + M_5'''T_{11}T_{13} + M_1'''T_{22}T_{12} + M_2'''T_{11}T_{12}]$$

(b)

M_1	$= N_1 + N_2 + N_3 + N_4$	M_2	$= N_5 + N_6 + N_7 + N_8$	M_3	$= N_9 + N_{10} + N_{11} + N_{12}$
M_4	$= N_{13} + N_{14} + N_{15} + N_{16}$	M_5	$= N_{17} + N_{18} + N_{19} + N_{20}$	M_6	$= N_{21} + N_{22} + N_{23} + N_{24}$
M_1'	$= N_1 - N_2 + N_3 - N_4$	M_2'	$= N_5 - N_6 + N_7 - N_8$	M_3'	$= N_9 - N_{10} + N_{11} - N_{12}$
M_4'	$= N_{13} - N_{14} + N_{15} - N_{16}$	M_5'	$= N_{17} - N_{18} + N_{19} - N_{20}$	M_6'	$= N_{21} - N_{22} + N_{23} - N_{24}$
M_1''	$= N_1 - N_2 - N_3 + N_4$	M_2''	$= N_5 - N_6 - N_7 + N_8$	M_3''	$= N_9 - N_{10} - N_{11} + N_{12}$
M_4''	$= N_{13} - N_{14} - N_{15} + N_{16}$	M_5''	$= N_{17} - N_{18} - N_{19} + N_{20}$	M_6''	$= N_{21} - N_{22} - N_{23} + N_{24}$
M_1'''	$= N_1 + N_2 - N_3 - N_4$	M_2'''	$= N_5 + N_6 - N_7 - N_8$	M_3'''	$= N_9 + N_{10} - N_{11} - N_{12}$
M_4'''	$= N_{13} + N_{14} - N_{15} - N_{16}$	M_5'''	$= N_{17} + N_{18} - N_{19} - N_{20}$	M_6'''	$= N_{21} + N_{22} - N_{23} - N_{24}$

From Eqs. (5) and (10) one finds

$$P_{iji'j'} = \sum_{r=1}^{\sigma} \mathcal{N}_r P_{iji'j'}^{(r)} , \qquad (11a)$$

where

$$P_{iji'j'}^{(r)} = \sum_{v_n \in V_r} T_{ij}^{(n)} T_{i'j'}^{(n)} . \qquad (11b)$$

Under the influence of the orientating operator $\hat{F}$ the number of different N_n equals the number of right cosets, σ, of the subgroup $F_1 \subset O$; σ must be a divisor of 24. This simplifies the expressions of the IP and generally reduces the number of independent IP's from 21 to a smaller number.

The effect of $\hat{F}$ on orientations v_n and $\hat{iv}_n$ may be different and different populations for the two orientations may result. Thus the inversion $\hat{i}$ cannot be omitted and the effect of the orientating operator $\hat{F}$ should be treated in the point group O_h. Since the Raman tensor is invariant under inversion, an orientation v_n can always be con-

sidered together with its partner $\hat{iv}_n$, and the population number is taken as the sum of the populations of v_n and $\hat{iv}_n$. Therefore, it is still possible to consider only the smaller cubic point group O. The subgroup $F_1 \subset O$ as defined in the preceding section is a *representative* of the corresponding subgroups $F_1' \subset O_h$ to which the orientating operator really belongs (see Table II).

For a general Raman tensor $\underline{T}^{(1)}$ of the defect and for given rotation $R_p \in O$ one finds [see also Eq. (6)]

$$R_p(T_{ij}^{(1)}T_{i'j'}^{(1)}) = K T_{st}^{(1)} T_{s't'}^{(1)} , \qquad (12a)$$

in which the rotation relates the sets of indices (i, j, i', j') and (s, t, s', t') to each other, and $K = +1$ or -1. If Eq. (12a) is determined for a rotation $R_p \in F_1$, it can be demonstrated that

$$P_{iji'j'} = K P_{sts't'} . \qquad (12b)$$

Furthermore, it can be shown that if for a general Raman tensor

$$P_{iji'j'}^{(1)} = 0 , \qquad (12c)$$

TABLE IV. (a) Right cosets of the 11 representative symmetries $F_1 \subset O$ (see Table II) of the orientating operator $\hat{F}$, using the identifying numbers of the elements of the cubic group as given in Table I. The orientations corresponding to group elements in the same coset possess the same population numbers. The subscripts identify the different right cosets. (b) Same as (a) but for the left cosets of the defect symmetry group $O_1 \subset O$. The orientations corresponding to group elements in the same coset are in fact identical and as a trivial result possess the same population numbers. The subscripts identify the different left cosets.

(a)

F_1	The Right Cosets of F_1
C_1	1 2 3 4 5 6 7 8 9 10 11 12 13 14 15 16 17 18 19 20 21 22 23 24
$C_2[100]$	$\{1,3\}_1$ $\{2,4\}_2$ $\{5,7\}_3$ $\{6,8\}_4$ $\{9,11\}_5$ $\{10,12\}_6$ $\{13,15\}_7$ $\{14,16\}_8$ $\{17,19\}_9$ $\{18,20\}_{10}$ $\{21,23\}_{11}$ $\{22,24\}_{12}$
$C_2[011]$	$\{1,11\}_1$ $\{2,10\}_2$ $\{3,9\}_3$ $\{4,12\}_4$ $\{5,23\}_5$ $\{6,22\}_6$ $\{7,21\}_7$ $\{8,24\}_8$ $\{13,19\}_9$ $\{14,18\}_{10}$ $\{15,17\}_{11}$ $\{16,20\}_{12}$
$D_2[100]$	$\{1,2,3,4\}_1$ $\{5,6,7,8\}_2$ $\{9,10,11,12\}_3$ $\{13,14,15,16\}_4$ $\{17,18,19,20\}_5$ $\{21,22,23,24\}_6$
$D_2[011]$	$\{1,3,9,11\}_1$ $\{2,4,10,12\}_2$ $\{5,7,21,23\}_3$ $\{6,8,22,24\}_4$ $\{13,15,17,19\}_5$ $\{14,16,18,20\}_6$
$C_3[111]$	$\{1,17,21\}_1$ $\{2,19,24\}_2$ $\{3,20,22\}_3$ $\{4,18,23\}_4$ $\{5,9,13\}_5$ $\{6,12,15\}_6$ $\{7,10,16\}_7$ $\{8,11,14\}_8$
$D_3[111]$	$\{1,5,9,13,17,21\}_1$ $\{2,6,12,15,19,24\}_2$ $\{3,8,11,14,20,22\}_3$ $\{4,7,10,16,18,23\}_4$
$C_4[100]$	$\{1,3,10,12\}_1$ $\{2,4,9,11\}_2$ $\{5,7,22,24\}_3$ $\{6,8,21,23\}_4$ $\{13,15,18,20\}_5$ $\{14,16,17,19\}_6$
$D_4[100]$	$\{1,2,3,4,9,10,11,12\}_1$ $\{5,6,7,8,21,22,23,24\}_2$ $\{13,14,15,16,17,18,19,20\}_3$
T	$\{1,2,3,4,17,18,19,20,21,22,23,24\}_1$ $\{5,6,7,8,9,10,11,12,13,14,15,16\}_2$
O	$\{1,2,3,4,5,6,7,8,9,10,11,12,13,14,15,16,17,18,19,20,21,22,23,24\}$

(b)

O_1	The Left Cosets of O_1
C_1	1 2 3 4 5 6 7 8 9 10 11 12 13 14 15 16 17 18 19 20 21 22 23 24
$C_2[010]$	$\{1,4\}_1$ $\{2,3\}_2$ $\{5,7\}_3$ $\{6,8\}_4$ $\{9,10\}_5$ $\{11,12\}_6$ $\{13,16\}_7$ $\{14,15\}_8$ $\{17,18\}_9$ $\{19,20\}_{10}$ $\{21,23\}_{11}$ $\{22,24\}_{12}$
$C_2[110]$	$\{1,6\}_1$ $\{2,5\}_2$ $\{3,8\}_3$ $\{4,7\}_4$ $\{9,24\}_5$ $\{10,23\}_6$ $\{11,22\}_7$ $\{12,21\}_8$ $\{13,19\}_9$ $\{14,20\}_{10}$ $\{15,17\}_{11}$ $\{16,18\}_{12}$
$D_2[100]$	$\{1,2,3,4\}_1$ $\{5,6,7,8\}_2$ $\{9,10,11,12\}_3$ $\{13,14,15,16\}_4$ $\{17,18,19,20\}_5$ $\{21,22,23,24\}_6$
$D_2[110]$	$\{1,2,5,6\}_1$ $\{3,4,7,8\}_2$ $\{9,12,21,24\}_3$ $\{10,11,22,23\}_4$ $\{13,15,17,19\}_5$ $\{14,16,18,20\}_6$
$C_3[111]$	$\{1,17,21\}_1$ $\{2,18,22\}_2$ $\{3,19,23\}_3$ $\{4,20,24\}_4$ $\{5,9,13\}_5$ $\{6,10,14\}_6$ $\{7,11,15\}_7$ $\{8,12,16\}_8$
$D_3[111]$	$\{1,5,9,13,17,21\}_1$ $\{2,6,10,14,18,22\}_2$ $\{3,7,11,15,19,23\}_3$ $\{4,8,12,16,20,24\}_4$
$C_4[001]$	$\{1,2,7,8\}_1$ $\{3,4,5,6\}_2$ $\{9,12,22,23\}_3$ $\{10,11,21,24\}_4$ $\{13,15,18,20\}_5$ $\{14,16,17,19\}_6$
$D_4[001]$	$\{1,2,3,4,5,6,7,8\}_1$ $\{9,10,11,12,21,22,23,24\}_2$ $\{13,14,15,16,17,18,19,20\}_3$
T	$\{1,2,3,4,17,18,19,20,21,22,23,24\}_1$ $\{5,6,7,8,9,10,11,12,13,14,15,16\}_2$
O	$\{1,2,3,4,5,6,7,8,9,10,11,12,13,14,15,16,17,18,19,20,21,22,23,24\}$

then the total IP also equals zero:

$$P_{iji'j'} = 0 . \qquad (12d)$$

Together with Eq. (6) these rules [Eqs. (12)], which are proven in Appendix B, facilitate the calculation of the IP expressions. Table I shows all the matrices $\underline{R}_n \in O$ and the corresponding $\underline{T}^{(n)}$ tensors expressed in the lattice coordinates (x,y,z); they are numbered from 1 to 24. $\underline{T}^{(1)}$ is the Raman tensor belonging to an arbitrarily chosen initial orientation of the defect.

By using Table I and the rules mentioned above one can readily find the independent nonzero IP under a given orientating operator $\hat{F}$. For example, let us take C_{2v} symmetry for $\hat{F}$ with a main axis [100] and two reflection planes, (011) and (0$\bar{1}$1). Its representative point group is D_2 with the axes [100], [011], and [0$\bar{1}$1] (See Table II). We denote this by $C_{2v}[100](011,0\bar{1}1)$ and $D_2[100,011,0\bar{1}1]$, or simply by $C_{2v}(011)$ and $D_2[011]$. We will employ these simplified symbols from now on. The representative symmetry group $F_1 = D_2[011]$ contains the following operators:

$$F_1 = \{C_1, C_2^x, C_2^{\bar{y}z}, C_2^{yz}\} .$$

Consider in Table I the four symmetrical tensors corresponding to the four elements of F_1. The transformations of the T_{ij} are given by

$$
\begin{array}{lllllll}
C_1: & T_{11} & T_{22} & T_{33} & T_{12} & T_{13} & T_{23} \\
C_2^x: & T_{11} & T_{22} & T_{33} & -T_{12} & -T_{13} & T_{23} \\
C_2^{\bar{y}z}: & T_{11} & T_{33} & T_{22} & T_{13} & T_{12} & T_{23} \\
C_2^{yz}: & T_{11} & T_{33} & T_{22} & -T_{13} & -T_{12} & T_{23}
\end{array}
$$

It is readily verified that

$$P_{1112} = P_{2212} = P_{3312} = 0 ,$$

$$P_{1113} = P_{2213} = P_{3313} = 0 ,$$

$$P_{1223} = P_{1323} = 0 ,$$

$$P_{2222} = P_{3333} ,$$

$$P_{1212} = P_{1313} ,$$

$$P_{1122} = P_{1133} ,$$

$$P_{2223} = P_{3323} ,$$

and the remaining five IP's are independent. Thus, under

the operator $\hat{F}$ with $F_1 = D_2[011]$, only nine independent nonzero IP's are left. Similarly one can easily verify the statement made in Sec. I that there are only three independent nonzero IP's for $F_1 = T$, i.e., when the defects are equally distributed over a¹¹ their possible equivalent orientations.

The numbers of independent population numbers, σ, and of independent Raman intensity parameters IP, μ_{IP}, are given in Table II. If no additional information about the Raman tensor is available the number of independent elements, μ_T, is equal to 6. Taking into account that only the relative values of the N_n, T_{ij}, and IP are of interest, Eqs. (9) reduce to a set of $\mu_{IP} - 1$ equations containing $\sigma - 1 + \mu_T - 1$ unknowns (Table II). As is readily verified for all cases, too many unknowns occur and the set of equations cannot be solved. In principle, if $\mu_{IP} > \sigma$, it is possible to repeat these experiments with different population distributions N_n to obtain a sufficient number of independent equations, but this can hardly be performed in a practical experiment. If $\mu_{IP} \leq \sigma$ one can never solve Eqs. (9).

In the following sections we will discuss how to determine the symmetry of the defect and its mode representations on the basis of an inspection of the behavior of the IP without solving Eqs. (9), and we introduce the concept of *behavior type*. Once this is achieved the number of independent equations and the number of unknowns in Eqs. (9) will be further reduced, and in many cases the relative values of the population numbers N_n and of the Raman-tensor elements T_{ij} can be determined.

C. Influence of the symmetry of the defect on the preferential orientation process

Take a defect in an arbitrary initial orientation v_1 with symmetry point group $O_1 \subset O$ and denote the left cosets by [Table IV(b)]:

$$O_1, O_2, \ldots, O_{\sigma'} .$$

The number σ' is a divisor of 24. Using the homomorphic correspondence from the point group O to the orientation set V, one finds the corresponding sets of orientations:

$$V'_1, V'_2, \ldots, V'_{\sigma'} .$$

It is possible to prove (Appendix C) that if

$$v_p, v_q \in V'_r, \quad r = 1, 2, \ldots, \sigma' , \tag{13a}$$

the orientations v_p and v_q are in fact the same and as a trivial result possess the same population number:

$$N_p = N_q . \tag{13b}$$

Combining this result with the effect of the orientating operator $\hat{F}$ of a given symmetry F_1 (see Sec. II B), the number of independent population numbers is often reduced again. If two directions v_p and v_q, which turn out to be identical because of the defect symmetry O_1, correspond to different right cosets of F_1 these cosets correspond in fact to the same set of orientations, with the same population number. This can formally be expressed

as follows.

If the sets $S_r \subset O$,

$$S_1, S_2, \ldots, S_{\sigma''}$$

are constructed by right and left multiplications of each of the rotation operators $\hat{R}_n$ as follows:

$$S_r = F_1 \hat{R}_n O_1 , \tag{14}$$

and the corresponding subsets of orientations are denoted by

$$V''_1, V''_2, \ldots, V''_{\sigma''} ,$$

all of the orientations belonging to a same set V''_r, resulting from the action of $\hat{F}$ on a defect of symmetry O_1, will possess the same population number, i.e., if one has

$$v_p, v_q \in S''_r, \quad r = 1, 2, \ldots, \sigma'' \tag{15a}$$

then

$$N_p = N_q \equiv \mathcal{N}_r . \tag{15b}$$

One can easily obtain the S_n or V''_n from Tables IV(a) and IV(b). For example, take $F_1 = D_2[011]$ as the symmetry of the orientating operator and $O_1 = D_2[110]$ as the symmetry of the defect. Check Tables IV(a) and IV(b) to obtain the right cosets of F_1 and the left cosets of O_1. Then combining the left and right cosets, one obtains the set S_r:

$$S_1 = (1\ 2\ 3\ 4\ 5\ 6\ 7\ 8\ 9\ 10\ 11\ 12\ 21\ 22\ 23\ 24) ,$$

$$S_2 = (13\ 15\ 17\ 19) , \tag{16}$$

$$S_3 = (14\ 16\ 18\ 20) .$$

The numbers in expressions (16) correspond to the Raman tensors in Table I. Only three independent N_n are left. This can simplify the set of Eqs. (9) considerably, but can only be employed after identification of the symmetry of the defect.

D. Identification of the dynamical mode through a behavior-type analysis of the Raman IP's

1. Dynamical modes which can be distinguished by Raman experiments

The symmetry of a defect and the representation to which the mode belongs are reflected in the Raman tensor (see Table V). The symmetry also determines relations between the population numbers which result from an orientating operator $\hat{F}$ of a given symmetry (see Secs. II B and II C). However, only part of this information can be retrieved from the Raman scattering experiments. Moreover, it can be derived from the explicit expressions of the IP (Table III) that for any possible symmetry of the orientating operator $\hat{F}$ it is impossible to distinguish a defect with symmetry $O_1 = T$ from one with symmetry $O_1 = O$ by means of Raman scattering. One can also demonstrate that an orientating operator of tetrahedral (T) or cubic (O) symmetry will yield exactly the same information about the symmetry of any defect, and about its dynamical modes. Therefore, we shall not distinguish any more between these two point groups.

TABLE V. Symmetric Raman tensors for the dynamical modes which can occur for defects in a cubic crystal structure for each of the 33 essentially different defect symmetry groups. The tensors have been transformed from the local reference frame (x', y', z') of the defect, to the crystal reference frame (x, y, z). The directions of the local axes are given in the Table. The notation of the tensor elements is mainly taken from Ref. 1, and their explicit expressions are given in the footnote of this table.

Defect symmetry	Raman active modes
The local frame	Raman tensors
C_1	$A(x',y',z';R_{x'},R_{y'},R_{z'})$
S_2	$A_g(R_{x'},R_{y'},R_{z'})$
$x' \parallel [100]$ $y' \parallel [010]$ $z' \parallel [001]$	$\begin{pmatrix} a_1 & d & f' \\ d & a_2 & f \\ f' & f & a_3 \end{pmatrix}$
$C_2[010]$ $C_{1h}(010)$ $C_{2h}[010]$	$A(y';R_{y'})$ $B(x',z';R_{x'},R_{z'})$ $A'(x',z';R_{y'})$ $A''(y';R_{x'},R_{z'})$ $A_g(R_{y'})$ $B_g(R_{x'},R_{z'})$
$x' \parallel [100]$ $y' \parallel [010]$ $z' \parallel [001]$	$\begin{pmatrix} a_1 & & f' \\ & a_2 & \\ f' & & a_3 \end{pmatrix}$ $\begin{pmatrix} & d & \\ d & & f \\ & f & \end{pmatrix}$
$C_2[110]$ $C_{1h}(110)$ $C_{2h}[110]$	$A(y';R_{y'})$ $B(x',z';R_{x'},R_{z'})$ $A'(x',z';R_{y'})$ $A''(y';R_{x'},R_{z'})$ $A_g(R_{y'})$ $B_g(R_{x'},R_{z'})$
$x' \parallel [1\bar{1}0]$ $y' \parallel [110]$ $z' \parallel [001]$	$\begin{pmatrix} a & -c & \frac{1}{\sqrt{2}}f' \\ -c & a & -\frac{1}{\sqrt{2}}f' \\ \frac{1}{\sqrt{2}}f' & -\frac{1}{\sqrt{2}}f' & a_3 \end{pmatrix}$ $\begin{pmatrix} d & & \frac{1}{\sqrt{2}}f \\ & -d & \frac{1}{\sqrt{2}}f \\ \frac{1}{\sqrt{2}}f & \frac{1}{\sqrt{2}}f & \end{pmatrix}$
$D_2[100,010,001]$ $C_{2v}[001](100,010)$ $D_{2h}[001,100,010]$	A $B_1(z';R_{z'})$ $B_2(y';R_{y'})$ $B_3(x';R_{x'})$ $A_1(z')$ $A_2(R_{z'})$ $B_1(x';R_{y'})$ $B_2(y';R_{x'})$ A_g $B_{1g}(R_{z'})$ $B_{2g}(R_{y'})$ $B_{3g}(R_{x'})$
$x' \parallel [100]$ $y' \parallel [010]$ $z' \parallel [001]$	$\begin{pmatrix} a_1 & & \\ & a_2 & \\ & & a_3 \end{pmatrix}$ $\begin{pmatrix} & d & \\ d & & \\ & & \end{pmatrix}$ $\begin{pmatrix} & & f' \\ & & \\ f' & & \end{pmatrix}$ $\begin{pmatrix} & & \\ & & f \\ & f & \end{pmatrix}$
$D_2[001,110,1\bar{1}0]$ $C_{2v}[001](110,1\bar{1}0)$ $D_{2h}[001,110,1\bar{1}0]$	A $B_1(z';R_{z'})$ $B_2(y';R_{y'})$ $B_3(x';R_{x'})$ $A_1(z')$ $A_2(R_{z'})$ $B_1(x';R_{y'})$ $B_2(y';R_{x'})$ A_g $B_{1g}(R_{z'})$ $B_{2g}(R_{y'})$ $B_{3g}(R_{x'})$
$x' \parallel [1\bar{1}0]$ $y' \parallel [110]$ $z' \parallel [001]$	$\begin{pmatrix} a & -c & \\ -c & a & \\ & & a_3 \end{pmatrix}$ $\begin{pmatrix} d & & \\ & -d & \\ & & \end{pmatrix}$ $\frac{1}{\sqrt{2}}\begin{pmatrix} & & f' \\ & & -f' \\ f' & -f' & \end{pmatrix}$ $\frac{1}{\sqrt{2}}\begin{pmatrix} & & f \\ & & f \\ f & f & \end{pmatrix}$
$C_{2v}[1\bar{1}0](110,001)$	$A_1(z')$ $B_1(x';R_{y'})$ $B_2(y';R_{x'})$ $A_2(R_{z'})$
$x' \parallel [110]$ $y' \parallel [001]$ $z' \parallel [1\bar{1}0]$	$\begin{pmatrix} a & -c' & \\ -c' & a & \\ & & a_3 \end{pmatrix}$ $\begin{pmatrix} f' & & \\ & -f' & \\ & & \end{pmatrix}$ $\frac{1}{\sqrt{2}}\begin{pmatrix} & & f \\ & & -f \\ f & -f & \end{pmatrix}$ $\frac{1}{\sqrt{2}}\begin{pmatrix} & & d \\ & & d \\ d & d & \end{pmatrix}$
$C_3[111]$ $S_6[111]$	$A(z';R_{z'})$ $E(x';R_{x'})$ $E(y';R_{y'})$ $A_g(R_{z'})$ $E_g^{(1)}(R_{x'})$ $E_g^{(2)}(R_{y'})$
$x' \parallel [1\bar{1}0]$ $y' \parallel [11\bar{2}]$ $z' \parallel [111]$	$\begin{pmatrix} a' & b' & b' \\ b' & a' & b' \\ b' & b' & a' \end{pmatrix}$ $\begin{pmatrix} b_{11} & b_{12} & b_{13} \\ b_{12} & b_{22} & b_{23} \\ b_{13} & b_{23} & b_{33} \end{pmatrix}$ $\begin{pmatrix} c_{11} & c_{12} & c_{13} \\ c_{12} & c_{22} & c_{23} \\ c_{13} & c_{23} & c_{33} \end{pmatrix}$
$D_3[111,1\bar{1}0,01\bar{1},10\bar{1}]$ $D_{3d}[111,1\bar{1}0,1\bar{1}0,10\bar{1}]$	A_1 $E(x';R_{x'})$ $E(y';R_{y'})$ A_{1g} $E_g^{(1)}(R_{x'})$ $E_g^{(2)}(R_{y'})$
$x' \parallel [1\bar{1}0]$ $y' \parallel [11\bar{2}]$ $z' \parallel [111]$	$\begin{pmatrix} a' & b' & b' \\ b' & a' & b' \\ b' & b' & a' \end{pmatrix}$ $\begin{pmatrix} h' & -2g' & g' \\ -2g' & h' & g' \\ g' & g' & -2h' \end{pmatrix}$ $\sqrt{3}\begin{pmatrix} -h' & & g' \\ & h' & -g' \\ g' & -g' & \end{pmatrix}$
$C_{3v}[111](1\bar{1}0,1\bar{1}0,10\bar{1})$	$A_1(z')$ $E(y';R_{x'})$ $E(x';R_{y'})$
$x' \parallel [1\bar{1}0]$ $y' \parallel [11\bar{2}]$ $z' \parallel [111]$	$\begin{pmatrix} a' & b' & b' \\ b' & a' & b' \\ b' & b' & a' \end{pmatrix}$ $\begin{pmatrix} d' & -2e' & e' \\ -2e' & d' & e' \\ e' & e' & -2d' \end{pmatrix}$ $\sqrt{3}\begin{pmatrix} d' & & -e' \\ & -d' & e' \\ -e' & e' & \end{pmatrix}$

TABLE V. (*Continued.*)

Defect symmetry	Raman active modes
The local frame	Raman tensors

$C_4[001]$	A(z';$R_{z'}$)	B	E(x';$R_{x'}$)	E(y';$R_{y'}$)	
$S_4[001]$	A($R_{z'}$)	B(z')	E(x';$R_{x'}$)	E(y';$R_{y'}$)	
$C_{4h}[001]$	A_g($R_{z'}$)	B_g	$E_g^{(1)}$($R_{x'}$)	$E_g^{(2)}$($R_{y'}$)	

$x' \parallel [100]$
$y' \parallel [010]$
$z' \parallel [001]$

$$\begin{pmatrix} a & & \\ & a & \\ & & a_3 \end{pmatrix} \quad \begin{pmatrix} c & d & \\ d & -c & \\ & & \end{pmatrix} \quad \frac{1}{\sqrt{2}}\begin{pmatrix} & & f' \\ & & f \\ f' & f & \end{pmatrix} \quad \frac{1}{\sqrt{2}}\begin{pmatrix} & & -f \\ & & f' \\ -f & f' & \end{pmatrix}$$

$D_4[001,100,010,110,1\bar{1}0]$	A_1	B_1	B_2	E(x';$R_{x'}$)	E(y';$R_{y'}$)
$D_{4h}[001,100,010,110,1\bar{1}0]$	A_{1g}	B_{1g}	B_{2g}	$E_g^{(1)}$($R_{x'}$)	$E_g^{(2)}$($R_{y'}$)
$D_{2d}[001,100,010](110,1\bar{1}0)$	A_1	B_1	$B_2(z')$	E(x';$R_{x'}$)	E(y';$R_{y'}$)

$x' \parallel [100]$
$y' \parallel [010]$
$z' \parallel [001]$

$$\begin{pmatrix} a & & \\ & a & \\ & & a_3 \end{pmatrix} \quad \begin{pmatrix} c & & \\ & -c & \\ & & \end{pmatrix} \quad \begin{pmatrix} & d & \\ d & & \\ & & \end{pmatrix} \quad \begin{pmatrix} & & \\ & & f \\ & f & \end{pmatrix} \quad \begin{pmatrix} & & -f \\ & & \\ -f & & \end{pmatrix}$$

$D_{2d}[001,110,1\bar{1}0](100,010)$	A_1	$B_2(z')$	B_1	E(x';$R_{x'}$)	E(y';$R_{y'}$)

$x' \parallel [100]$
$y' \parallel [010]$
$z' \parallel [001]$

$$\begin{pmatrix} a & & \\ & a & \\ & & a_3 \end{pmatrix} \quad \begin{pmatrix} d & & \\ & -d & \\ & & \end{pmatrix} \quad \begin{pmatrix} & -c & \\ -c & & \\ & & \end{pmatrix} \quad \frac{1}{\sqrt{2}}\begin{pmatrix} & & f \\ & & f \\ f & f & \end{pmatrix} \quad \frac{1}{\sqrt{2}}\begin{pmatrix} & & -f \\ & & f \\ -f & f & \end{pmatrix}$$

$C_{4v}[001](100,010,110,1\bar{1}0)$	$A_1(z')$	B_1	B_2	E(y';$R_{x'}$)	E(x';$R_{y'}$)

$x' \parallel [100]$
$y' \parallel [010]$
$z' \parallel [001]$

$$\begin{pmatrix} a & & \\ & a & \\ & & a_3 \end{pmatrix} \quad \begin{pmatrix} c & & \\ & -c & \\ & & \end{pmatrix} \quad \begin{pmatrix} & d & \\ d & & \\ & & \end{pmatrix} \quad \begin{pmatrix} & & \\ & & f' \\ & f' & \end{pmatrix} \quad \begin{pmatrix} & & f' \\ & & \\ f' & & \end{pmatrix}$$

T	A	$E^{(1)}$	$E^{(2)}$	T(x';$R_{x'}$)	T(y';$R_{y'}$)	T(z';$R_{z'}$)
T_h	A_g	$E_g^{(1)}$	$E_g^{(2)}$	$T_g^{(1)}$ ($R_{x'}$)	$T_g^{(2)}$($R_{y'}$)	$T_g^{(3)}$($R_{z'}$)

$x' \parallel [100]$
$y' \parallel [010]$
$z' \parallel [001]$

$$\begin{pmatrix} a & & \\ & a & \\ & & a \end{pmatrix} \quad 2\begin{pmatrix} g_1 & & \\ & g_2 & \\ & & -g \end{pmatrix} \quad -\frac{\sqrt{3}}{\sqrt{2}}\begin{pmatrix} b & & \\ & c & \\ & & d \end{pmatrix} \quad \begin{pmatrix} & & \\ & & f \\ & f & \end{pmatrix} \quad \begin{pmatrix} & & f \\ & & \\ f & & \end{pmatrix} \quad \begin{pmatrix} & f & \\ f & & \\ & & \end{pmatrix}$$

O	A_1	$E^{(1)}$	$E^{(2)}$	$T_2^{(1)}$	$T_2^{(2)}$	$T_2^{(3)}$
T_d	A_1	$E^{(1)}$	$E^{(2)}$	$T_2(x')$	$T_2(y')$	$T_2(z')$
O_h	A_{1g}	$E_g^{(1)}$	$E_g^{(2)}$	$T_{2g}^{(1)}$	$T_{2g}^{(2)}$	$T_{2g}^{(3)}$

$x' \parallel [100]$
$y' \parallel [010]$
$z' \parallel [001]$

$$\begin{pmatrix} a & & \\ & a & \\ & & a \end{pmatrix} \quad 2\sqrt{2}\begin{pmatrix} g & & \\ & g & \\ & & -2g \end{pmatrix} \quad 2\sqrt{6}\begin{pmatrix} -g & & \\ & g & \\ & & \end{pmatrix} \quad \begin{pmatrix} & & \\ & & f \\ & f & \end{pmatrix} \quad \begin{pmatrix} & & f \\ & & \\ f & & \end{pmatrix} \quad \begin{pmatrix} & f & \\ f & & \\ & & \end{pmatrix}$$

The expressions of the symbols of the tensor elements :

In trigonal and tetragonal classes :

$$a = \tfrac{1}{2}(x'x' + y'y') \qquad c = \tfrac{1}{2}(x'x' - y'y') \qquad d = \tfrac{1}{2}(x'y' + y'x')$$

In cubic classes :

$$a = \tfrac{1}{3}(x'x' + y'y' + z'z') \qquad c = \tfrac{1}{6}(z'z' - x'x') \qquad d = \tfrac{1}{6}(x'x' - y'y')$$

In all symmetry groups :

$$b = \tfrac{1}{6}(y'y' - z'z') \qquad g = \tfrac{1}{12\sqrt{2}}(x'x' + y'y' - 2z'z') \qquad f = \tfrac{1}{2}(y'z' + z'y')$$

$$h = \tfrac{\sqrt{3}}{12\sqrt{2}}(x'x' - y'y') \qquad g_1 = \tfrac{1}{12\sqrt{2}}(2x'x' - y'y' + z'z') \qquad g_2 = g - g_1$$

$$a_1 = x'x' \qquad a_2 = y'y' \qquad a_3 = z'z'$$

$$f' = \tfrac{1}{2}(x'z' + z'x') \qquad c' = \tfrac{1}{2}(z'z' - x'x') \qquad a' = \tfrac{2}{3}a + \tfrac{1}{3}a_3$$

$$b' = -\tfrac{1}{3}a + \tfrac{1}{3}a_3 \qquad d' = \tfrac{1}{3}d + \tfrac{\sqrt{2}}{3}f' \qquad e' = \tfrac{1}{3}d - \tfrac{\sqrt{2}}{6}f'$$

$$g' = \tfrac{1}{3}c - \tfrac{\sqrt{2}}{6}f \qquad\qquad h' = \tfrac{1}{3}c + \tfrac{\sqrt{2}}{3}f$$

$$b_{11} = \tfrac{\sqrt{2}}{3}c + \tfrac{\sqrt{6}}{3}d + \tfrac{\sqrt{3}}{3}f' + \tfrac{1}{3}f \qquad b_{22} = \tfrac{\sqrt{2}}{3}c - \tfrac{\sqrt{6}}{3}d - \tfrac{\sqrt{3}}{3}f' + \tfrac{1}{3}f \qquad b_{33} = -b_{11} - b_{22}$$

$$b_{23} = \tfrac{\sqrt{2}}{3}c + \tfrac{\sqrt{6}}{3}d - \tfrac{\sqrt{3}}{6}f' - \tfrac{1}{6}f \qquad b_{13} = \tfrac{\sqrt{2}}{3}c - \tfrac{\sqrt{6}}{3}d + \tfrac{\sqrt{3}}{6}f' - \tfrac{1}{6}f \qquad b_{12} = -b_{23} - b_{13}$$

$$c_{11} = \tfrac{\sqrt{2}}{3}d + \tfrac{\sqrt{6}}{3}c + \tfrac{\sqrt{3}}{3}f + \tfrac{1}{3}f' \qquad c_{22} = \tfrac{\sqrt{2}}{3}d - \tfrac{\sqrt{6}}{3}c - \tfrac{\sqrt{3}}{3}f + \tfrac{1}{3}f' \qquad c_{33} = -c_{11} - c_{22}$$

$$c_{23} = \tfrac{\sqrt{2}}{3}d + \tfrac{\sqrt{6}}{3}c - \tfrac{\sqrt{3}}{6}f - \tfrac{1}{6}f' \qquad c_{13} = \tfrac{\sqrt{2}}{3}d - \tfrac{\sqrt{6}}{3}c + \tfrac{\sqrt{3}}{6}f - \tfrac{1}{6}f' \qquad c_{12} = -c_{13} - c_{23}$$

Even when this is taken into account one can verify that different modes corresponding to the same defect symmetry cannot be distinguished from one another, even when a full set of 21 IP's is available. This results partly from an internal symmetry of Eqs. (9) (see Appendix D) and partly from the explicit expressions of the IP for each of the defect symmetries. The following modes cannot be distinguished from each other.

(i) The B_1, B_2, and B_3 modes of a defect with symmetry $O_1 = D_2[100]$. The three modes possess, in general, different frequencies.

(ii) The components of a twofold-degenerate mode, an E mode, yield the same contribution to the Raman IP. In most circumstances the two modes cannot be measured separately while possessing the same frequency. However, the rule can be useful when a perturbation lifts this degeneracy, e.g., the perturbation induced by a uniaxial stress on the crystal. In the same way the three degenerate modes of a T representation contribute equally to the IP.

Taking into account the above remarks and the neglect of inversion symmetry, we conclude that of 124 possible dynamical modes with different symmetry properties only 25 sets can be distinguished from one another on the basis of Raman experiments on preferentially orientated defects. We have listed these sets in Table VI and will indicate them by 25 so-called *representative modes*.

When the analysis of the IP is considered for an experiment in which only one mode of a defect is studied, additional limitations occur. We have checked that the representative modes within the following sets cannot be distinguished from each other even by solving Eqs. (9):

$$\{D_2[100]{:}B_1, \ C_4{:}E, \ D_4{:}B_2, \ E\} \ , \tag{17a}$$

$$\{D_2[110]{:}B_1, \ D_4{:}B_1\} \ , \tag{17b}$$

$$\{C_3{:}A, \ D_3{:}A_1\} \ , \tag{17c}$$

$$\{C_4{:}A, \ D_4{:}A_1\} \ . \tag{17d}$$

This follows from an inspection of the IP expressions (5) explicitly taking into account the population numbers and the Raman-tensor components. Thus only 19 sets of representative modes can possibly be distinguished in a single-mode analysis.

In this section we have not considered whether Eqs. (9) can actually be solved, i.e., whether a sufficient number of independent IP's exists for determination of the unknown population numbers N_n and the elements T_{ij} of the Raman tensor. For some of the representative modes Eqs. (9) cannot be solved for any symmetry F_1 of the orientating operator $\hat{F}$, and this puts an additional limit to our analysis, as will be demonstrated now in the following section (Sec. II D 2).

2. Symmetry-imposed properties of the Raman IP's: Behavior type

In order to determine the population number N_n and the elements of the Raman tensor it is necessary to solve the set of Eqs. (9). However, these are cubic equations, with a high number of unknowns. Furthermore, because of the insufficient precision of the experimental results it

is often hard to proceed along this way. Moreover, for several of the representative modes it is not possible to find the solutions.

Therefore, we will try to determine the representative modes on the basis of a *direct inspection of relations existing between the IP's*. As mentioned above in Sec. II D 1, part of the symmetry-imposed information contained in the Raman tensor of the mode and the population numbers N_n is reflected in these parameters. In many cases this information can be expressed by means of relatively simple relations between the IP's, which are easy to discern in the experimental data. We have systematically inspected the occurrence of the following types of IP relations:

$$x_i = 0 \ , \tag{18a}$$

$$x_i \leq 0 \ , \tag{18b}$$

$$x_i = c x_j \ , \tag{18c}$$

$$x_i = c(x_j + x_k) \ , \tag{18d}$$

$$x_i / x_j = c(x_k / x_h) \ , \tag{18e}$$

$$x_i / x_j = c(x_k / x_h)^{1/2} \ , \tag{18f}$$

where x_i, x_j, x_k, x_h represent specific IP's, and c is a positive or negative integer or half integer. For a given set of 21 IP's one can check which of the IP relations of the types shown above are fulfilled. These IP relations define a so-called behavior type (BT) of the set of IP's.

From the explicit expressions of IP's for all of the possible representative modes, and after applying a given orientating operator $\hat{F}$, we have determined that 65 different BT's can occur. Their characteristic IP relations are listed in Table VII: The IP's equal to zero [(18a)] and the relations between two IP's [(18c)] can be found directly in the table; the other relations [(18b)], (18d)–(18f)] are given in the footnotes of the table and are referred to in the last column. If two BT's differ from each other only by the relations between three or more IP's, as given in the last column of Table VII, they are assigned the same number but with an additional letter, e.g., BT nos. 23a and 23b. Table VIII indicates the BT for each of the modes and all possible symmetries of the orientating operator $\hat{F}$, using the definition of the BT as given in Table VII.

If one considers a given defect symmetry O_1, the BT which is found for $F_1 = C_1$ (first column of Table VIII) is the *minimum* BT for this defect, i.e., all of the IP relations which are valid in this BT are also obeyed for higher symmetries F_1 of the orientating operator $\hat{F}$. This BT is induced purely by the symmetry of the defect. In a similar way the BT for a given F_1 and for the defect symmetry $O_1 = C_1$ (first row in Table VIII) is characteristic for the symmetry of the orientating operator, and the IP of a defect with a higher symmetry O_1 will obey the IP relations of this BT. The latter IP relations can be used in an experiment to test the symmetry F_1 of the orientating operator. In addition to the sets considered above [Eqs. (17)] the following sets of modes possess the same BT for any symmetry F_1 (see Table VIII):

TABLE VI. Classification of the dynamical modes which can occur for defects in a cubic crystal according to the 25 representative modes which can be distinguished by Raman scattering experiments. The representative modes are given an identifying number for reference in Tables VIII, IX, and XIII(b).

Representative Mode	Number of modes	Dynamical modes
1 C_1:A	2	C_1:A S_2:A_g
2 $C_2[010]$:A	3	$C_2[010]$:A $C_{1h}(010)$:A' $C_{2h}[010]$:A_g
3 $C_2[010]$:B	3	$C_2[010]$:B $C_{1h}(010)$:A'' $C_{2h}[010]$:B_g
4 $C_2[110]$:A	3	$C_2[110]$:A $C_{1h}(110)$:A' $C_{2h}[110]$:A_g
5 $C_2[110]$:B	3	$C_2[110]$:B $C_{1h}(110)$:A'' $C_{2h}[110]$:B_g
6 $D_2[100]$:A	3	$D_2[100]$:A $C_{2v}(100)$:A_1 $D_{2h}[100]$:A_g
7 $D_2[100]$:B_1	9	$D_2[100]$:B_1,B_2,B_3 $C_{2v}(100)$:A_2,B_1,B_2 $D_{2h}[100]$:B_{1g},B_{2g},B_{3g}
8 $D_2[110]$:A	4	$D_2[110]$:A $C_{2v}(110)$:A_1 $D_{2h}[110]$:A_g $C_{2v}[1\bar{1}0]$:A_1
9 $D_2[110]$:B_1	4	$D_2[110]$:B_1 $C_{2v}(110)$:A_2 $D_{2h}[110]$:B_{1g} $C_{2v}[1\bar{1}0]$:B_1
10 $D_2[110]$:B_2	4	$D_2[110]$:B_2 $C_{2v}(110)$:B_1 $D_{2h}[110]$:B_{2g} $C_{2v}[1\bar{1}0]$:B_2
11 $D_2[110]$:B_3	4	$D_2[110]$:B_3 $C_{2v}(110)$:B_2 $D_{2h}[110]$:B_{3g} $C_{2v}[1\bar{1}0]$:A_2
12 $C_3[111]$:A	2	C_3:A S_6:A_g
13 $C_3[111]$:E	4	C_3:E S_6:E_g
14 $D_3[111]$:A_1	3	D_3:A_1 D_{3d}:A_{1g} C_{3v}:A_1
15 $D_3[111]$:E	6	D_3:E D_{3d}:E_g C_{3v}:E
16 $C_4[001]$:A	3	C_4:A S_4:A C_{4h}:A_g
17 $C_4[001]$:B	3	C_4:B S_4:B C_{4h}:B_g
18 $C_4[001]$:E	6	C_4E S_4:E C_{4h}:E_g
19 $D_4[001]$:A_1	5	D_4:A_1 D_{4h}:A_{1g} $D_{2d}[001]$:A_1 $D_{2d}[110]$:A_1 C_{4v}:A_1
20 $D_4[001]$:B_1	5	D_4:B_1 D_{4h}:B_{1g} $D_{2d}[001]$:B_1 $D_{2d}[110]$:B_2 C_{4v}:B_1
21 $D_4[001]$:B_2	5	D_4:B_2 D_{4d}:B_{2g} $D_{2d}[001]$:B_2 $D_{2d}[110]$:B_1 C_{4v}:B_2
22 $D_4[001]$:E	10	D_4:E D_{4h}:E_g $D_{2d}[001]$:E $D_{2d}[110]$:E C_{4v}:E
23 T:A	5	T:A T_h:A_g O:A_1 T_d:A_1 O_h:A_{1g}
24 T:E	10	T:E T_h:E_g O:E T_d:E O_h:E_g
25 T:T	15	T:T T_h:T_g O:T_2 T_d:T_2 O_h:T_{2g}

$$\{C_1,A,\ C_2[110]{:}A\}\ , \tag{19a}$$

$$\{C_2[010]{:}B\ D_2[110]{:}B_2,\ B_3\}\ , \tag{19b}$$

$$\{D_2[100]{:}A,\ C_4{:}A\}\ . \tag{19c}$$

As a result only 15 sets of modes can be distinguished from one another by the single-mode BT analysis. In sets (19a) and (19c) it is possible to solve Eqs. (9) and to decide between the representative modes on the basis of the population numbers N_n and the elements T_{ij} of the Raman tensor. Solving Eqs. (9) is not possible for the modes in set (19b) and as a result it is impossible to decide between

them on the basis of Raman measurements on a single dynamical mode: This reduces the number of distinguishable sets of representative modes from 19 to 17. This number should be compared with 15 for the BT analysis.

As mentioned in Sec. II A only part of the subgroups of the cubic point group O were considered in our analysis, e.g., $D_4[100]$ for F_1 but not $D_4[001]$ and $D_4[010]$. It is relatively easy to derive the BT for such rotated subgroups from the BT listed in Table VII. A rotation from one subgroup to another by $\hat{R}_n \in O$ is equivalent to an inverse rotation by $\hat{R}\,_n^{-1}$ of the defects and their reference axes. The rotation of the defects need not be taken into account

TABLE VII. Sixty-five different BT's identified by a BT number in the first column are defined by relations of the type given in Eqs. (18) between the 21 IP's. The IP's which are zero and the relations between two IP's are given as the main BT. The relations between more than two IP's (the additional BT relations) are given in the footnotes of this table and are indicated in the last column. The equalities among the IP's existing for a given BT can be substituted into these additional relations. This often permits one to apply these relations even if the IP's which explicitly appear in them are not directly available from the experiment.

BT no.	Main BT relations			Additional BT relations[a]
1	$q_1\ q_2\ q_3\ r_1\ r_2\ r_3$	$s_1\ s_2\ s_3\ t_1\ t_2\ t_3$	$u_1\ u_2\ u_3\ v_1\ v_2\ v_3\ v_4\ v_5\ v_6$	−
2	$q_1\ q_2\ q_3\ r_1\ r_2\ r_3$	$s_1\ s_2\ s_3$	$u_1\ u_2\ u_3\ v_1\ v_2\ v_3\ v_4\ v_5\ v_6$	−
3		$s_1\ s_2\ s_3\ t_1\ t_2\ t_3$		−
4	$q_1\ q_2\ q_3\ r_1\ r_2\ r_3$	$s_1\ s_2\ s_3\ t_1\ t_2\ t_3$	$u_1\ u_2\ u_3\ v_1\ v_2\ v_3\ v_4\ v_5\ v_6$	1 2 3 4 5 6 10 13
5	$q_1\ q_2\ q_3\ r_1\ r_2\ r_3$			−
6		$s_1\ s_2\ s_3$		−
7	$q_1\ q_2\ q_3\ r_1\ r_2\ r_3$	$s_1\ s_2\ s_3$	$u_1\ u_2\ u_3\ v_1\ v_1\ v_3\ v_3\ v_5\ v_5$	12
8	$q_1\ q_2\ q_3\ r_1\ r_2\ r_3$			1 2 3 13
9	$q_1\ q_1\ q_1\ q_1\ q_1\ q_1$	$s_1\ s_1\ s_1\ t_1\ t_2\ t_3$	$u_1\ u_2\ u_3\ u_1\ u_1\ u_2\ u_2\ u_3\ u_3$	8
10	$q_1\ q_1\ q_1-\tfrac12 q_1-\tfrac12 q_1-\tfrac12 q_1$	$s_1\ s_1\ s_1\ t_1\ t_2\ t_3$	$u_1\ u_2\ u_3\ v_1\ v_2\ v_3\ v_4\ v_5\ v_6$	4 5 6
11	$q_1\ q_1\ q_1-\tfrac12 q_1-\tfrac12 q_1-\tfrac12 q_1$	$s_1\ s_1\ s_1\ t_1\ t_2\ t_3$	$u_1\ u_2\ u_3-\tfrac12 u_1-\tfrac12 u_1-\tfrac12 u_2-\tfrac12 u_2-\tfrac12 u_3-\tfrac12 u_3$	9
12	$q_1\ q_2\ q_3\ r_1\ r_2\ r_3$	$s_1\ s_2\ s_3$	$v_1\ -v_1\ v_3\ -v_3\ v_5\ -v_5$	1 2 3 11 13
13	$q_1\ q_1\ q_1\ q_1\ q_1\ q_1$			−
14	$q_1\ q_1\ q_1-\tfrac12 q_1-\tfrac12 q_1-\tfrac12 q_1$			−
15		$s_1\ s_1\ s_1$		−
16	$q_1\ q_2\ q_3\ r_1\ r_2\ r_3$	$s_1\ s_2\ s_3\ t_1$	$u_1\quad v_1\ v_2$	−
17	$q_1\ q_2\ q_3\ r_1\ r_2\ r_3$	$s_1\ s_2\ s_3$	$u_1\quad v_1\ v_2$	−
18		$s_1\ s_2\ s_3\ t_1$		−
19	$q_1\ q_2\ q_3\ r_1\ r_2\ r_3$	$s_1\ s_2\ s_3\ t_1$	$u_1\quad v_1\ v_2$	1 2 3 4 10 13
20	$q_1\ q_2\ q_3\ r_1\ r_2\ r_3$	$s_1\ s_2\ s_3$	$u_1\quad v_1\ v_1$	−
21	$q_1\ q_1\ q_1\ q_1\ q_1\ q_1$	$s_1\ s_1\ s_1\ t_1$	$u_1\quad u_1\ u_1$	8
22	$q_1\ q_1\ q_1-\tfrac12 q_1-\tfrac12 q_1-\tfrac12 q_1$	$s_1\ s_1\ s_1\ t_1$	$u_1\quad v_1\ v_2$	4
23a	$q_1\ q_1\ q_1-\tfrac12 q_1-\tfrac12 q_1-\tfrac12 q_1$	$s_1\ s_1\ s_1\ t_1$	$u_1\quad -\tfrac12 u_1-\tfrac12 u_1$	−
23b	$q_1\ q_1\ q_1-\tfrac12 q_1-\tfrac12 q_1-\tfrac12 q_1$	$s_1\ s_1\ s_1\ t_1$	$u_1\quad -\tfrac12 u_1-\tfrac12 u_1$	9
24	$q_1\ q_2\ q_3\ r_1\ r_2\ r_3$	$s_1\ s_2\ s_3$	$v_1\ -v_1$	1 2 3 11 13
25	$q_1\ q_2\ q_2\ r_1\ r_2\ r_2$	$s_1\ s_2\ s_2\ t_1\ t_2\ -t_2$	$u_1\ u_2\ -u_2\ v_1\ v_1\ v_3\ v_4\ -v_3\ -v_4$	−
26	$q_1\ q_2\ q_2\ r_1\ r_2\ r_2$	$s_1\ s_2\ s_2$	$u_1\ u_2\ -u_2\ v_1\ v_1\ v_3\ v_4\ -v_3\ -v_4$	−
27		$s_1\ s_2\ s_2\ t_1\ t_2\ -t_2$		−
28	$q_1\ q_2\ q_2\ r_1-\tfrac12 q_1-\tfrac12 q_1$	$s_1\ s_2\ s_2\ t_1\ t_2\ -t_2$	$u_1\ u_2\ -u_2-\tfrac12 u_1-\tfrac12 u_1\ v_3\ v_4\ -v_3\ -v_4$	2 5 7 10 13
29	$q_1\ q_2\ q_2\ r_1\ r_2\ r_2$			−
30		$s_1\ s_2\ s_2$		−
31	$q_1\ q_2\ q_2\ r_1\ r_2\ r_2$	$s_1\ s_2\ s_2$	$u_1\ u_2\ -u_2\ v_1\ v_1\ v_3\ v_3\ -v_3\ -v_3$	12
32	$q_1\ q_2\ q_2\ r_1-\tfrac12 q_1-\tfrac12 q_1$			2 7 13
33	$q_1\ q_1\ q_1\ q_1\ q_1\ q_1$	$s_1\ s_1\ s_1\ t_1\ t_2\ -t_2$	$u_1\ u_2\ -u_2\ u_1\ u_1\ u_2\ u_2\ -u_2\ -u_2$	8
34	$q_1\ q_1\ q_1-\tfrac12 q_1-\tfrac12 q_1-\tfrac12 q_1$	$s_1\ s_1\ s_1\ t_1\ t_2\ -t_2$	$u_1\ u_2\ -u_2-\tfrac12 u_2-\tfrac12 u_2\ v_3\ v_4\ -v_3\ -v_4$	5
35	$q_1\ q_1\ q_1-\tfrac12 q_1-\tfrac12 q_1-\tfrac12 q_1$	$s_1\ s_1\ s_1\ t_1\ t_2\ -t_2$	$u_1\ u_2\ -u_2-\tfrac12 u_1-\tfrac12 u_1-\tfrac12 u_2-\tfrac12 u_2\ \tfrac12 u_2\ \tfrac12 u_2$	9

because it is equivalent to a different choice of the original orientation v_1. A rotation $\widehat{R}_n^{-1}$ yields a permutation of the x, y, and z axes, and as a result a permutation of the IP occurs [see Eqs. (5) and (9)]. The permutation is such that in the short IP notation $q_i, r_i, s_i, \ldots$, introduced in Eqs. (8), only the lower indices are permuted, i.e., the permutation occurs between the q_i, between the r_i, and so on. It is evident that the representative modes can be distinguished from each other in the same way by a rotated F_1 as by the original one listed in the tables.

3. Combined analysis of several modes of the same point defect

Sometimes it is possible to detect several modes of the same defect and to analyze the IP of these modes simultaneously. If, for a given symmetry F_1, several modes of the same defect are found to possess a different BT, the symmetry O_1 of this defect can be determined more efficiently. For example, one can decide between the modes $C_1{:}A$ and $C_2[110]{:}A$ [see Eq. (19a)] if a second mode of

TABLE VII. (Continued.)

BT no.	Main BT relations					Additional BT relations[a]
36	$q_1\ q_2\ q_2$ $r_1-\tfrac{1}{2}q_1-\tfrac{1}{2}q_1$	$s_1\ s_2\ s_2$			$v_3\ \ -v_3\ \ -v_3\ \ v_3$	2 7 11 13
37	$q_1\ q_2\ q_3$ $r_1\ \ r_2\ \ r_3$	$s_1\ s_2\ s_3$				−
38a	$q_1\ q_2\ q_3$ $r_1\ \ r_2\ \ r_3$	$s_1\ s_2\ s_3$				1 2 3 10 13
38b	$q_1\ q_2\ q_3$ $r_1\ \ r_2\ \ r_3$	$s_1\ s_2\ s_3$				1 2 3 11 13
39	$q_1\ q_1\ q_1$ $q_1\ \ q_1\ \ q_1$	$s_1\ s_1\ s_1$				−
40	$q_1\ q_1\ q_1-\tfrac{1}{2}q_1-\tfrac{1}{2}q_1-\tfrac{1}{2}q_1$	$s_1\ s_1\ s_1$				−
41	$q_1\ q_2\ q_2$ $r_1\ \ r_2\ \ r_2$	$s_1\ s_2\ s_2\ t_1$	u_1	$v_1\ \ v_1$		−
42	$q_1\ q_2\ q_2$ $r_1\ \ r_2\ \ r_2$	$s_1\ s_2\ s_2$	u_1	$v_1\ \ v_1$		−
43		$s_1\ s_2\ s_2\ t_1$				−
44	$q_1\ q_2\ q_2$ $r_1-\tfrac{1}{2}q_1-\tfrac{1}{2}q_1$	$s_1\ s_2\ s_2\ t_1$	u_1	$-\tfrac{1}{2}u_1-\tfrac{1}{2}u_1$		2 7 10 13
45a	$q_1\ q_2\ q_2$ $r_1-\tfrac{1}{2}q_1-\tfrac{1}{2}q_1$	$s_1\ s_2\ s_2$				2 7 10 13
45b	$q_1\ q_2\ q_2$ $r_1-\tfrac{1}{2}q_1-\tfrac{1}{2}q_1$	$s_1\ s_2\ s_2$				2 7 11 13
46	$q_1\ q_1\ q_1$ $r_1\ \ r_1\ \ r_1$	$s_1\ s_1\ s_1\ t_1\ t_1\ t_1$	$u_1\ u_1\ \ u_1$	$v_1\ \ v_2\ \ v_2\ \ v_1\ \ v_1\ \ v_2$		−
47	$q_1\ q_1\ q_1$ $r_1\ \ r_1\ \ r_1$	$s_1\ s_1\ s_1$	$u_1\ u_1\ \ u_1$	$v_1\ \ v_2\ \ v_2\ \ v_1\ \ v_1\ \ v_2$		−
48		$s_1\ s_1\ s_1\ t_1\ t_1\ t_1$				−
49	$q_1\ q_1\ q_1-\tfrac{1}{2}q_1-\tfrac{1}{2}q_1-\tfrac{1}{2}q_1$	$s_1\ s_1\ s_1\ t_1\ t_1\ t_1$	$u_1\ u_1\ \ u_1$	$v_1\ \ v_2\ \ v_2\ \ v_1\ \ v_1\ \ v_2$		4 13
50	$q_1\ q_1\ q_1$ $r_1\ \ r_1\ \ r_1$					−
51	$q_1\ q_1\ q_1$ $r_1\ \ r_1\ \ r_1$	$s_1\ s_1\ s_1$	$u_1\ u_1\ \ u_1$	$v_1\ \ v_1\ \ v_1\ \ v_1\ \ v_1\ \ v_1$		−
52	$q_1\ q_1\ q_1$ $q_1\ \ q_1\ \ q_1$	$s_1\ s_1\ s_1\ t_1\ t_1\ t_1$	$u_1\ u_1\ \ u_1$	$u_1\ \ u_1\ \ u_1\ \ u_1\ \ u_1\ \ u_1$		8
53a	$q_1\ q_1\ q_1-\tfrac{1}{2}q_1-\tfrac{1}{2}q_1-\tfrac{1}{2}q_1$	$s_1\ s_1\ s_1\ t_1\ t_1\ t_1$	$u_1\ u_1$	$u_1-\tfrac{1}{2}u_1-\tfrac{1}{2}u_1-\tfrac{1}{2}u_1-\tfrac{1}{2}u_1-\tfrac{1}{2}u_1-\tfrac{1}{2}u_1$		−
53b	$q_1\ q_1\ q_1-\tfrac{1}{2}q_1-\tfrac{1}{2}q_1-\tfrac{1}{2}q_1$	$s_1\ s_1\ s_1\ t_1\ t_1\ t_1$	$u_1\ u_1$	$u_1-\tfrac{1}{2}u_1-\tfrac{1}{2}u_1-\tfrac{1}{2}u_1-\tfrac{1}{2}u_1-\tfrac{1}{2}u_1-\tfrac{1}{2}u_1$		9
54	$q_1\ q_1\ q_1-\tfrac{1}{2}q_1-\tfrac{1}{2}q_1-\tfrac{1}{2}q_1$	$s_1\ s_1\ s_1$		$v_1\ \ -v_1\ \ -v_1\ \ v_1\ \ v_1\ \ -v_1$		13
55	$q_1\ q_1\ q_1$ $r_1\ \ r_1\ \ r_1$	$s_1\ s_1\ s_1\ t_1\ t_1\ t_1$	$u_1\ u_1\ \ u_1$	$v_1\ \ v_1\ \ v_1\ \ v_1\ \ v_1\ \ v_1$		−
56	$q_1\ q_2\ q_2$ $r_1\ \ r_2\ \ r_2$	$s_1\ s_2\ s_2$		$v_1\ \ -v_1$		−
57a	$q_1\ q_2\ q_2$ $r_1-\tfrac{1}{2}q_1-\tfrac{1}{2}q_1$	$s_1\ s_2\ s_2$		$v_1\ \ -v_1$		2 7 10 13
57b	$q_1\ q_2\ q_2$ $r_1-\tfrac{1}{2}q_1-\tfrac{1}{2}q_1$	$s_1\ s_2\ s_2$		$v_1\ \ -v_1$		2 7 11 13
58	$q_1\ q_2\ q_2$ $r_1\ \ r_2\ \ r_2$	$s_1\ s_2\ s_2$				−
59	$q_1\ q_1\ q_1-\tfrac{1}{2}q_1-\tfrac{1}{2}q_1-\tfrac{1}{2}q_1$	$s_1\ s_1\ s_1$		$v_1\ \ -v_1$		−
60	$q_1\ q_1\ q_1$ $r_1\ \ r_1\ \ r_1$	$s_1\ s_1\ s_1$				−

[a]The numbers in this column indicate the following additional IP relations :

1 : $q_1 = -r_2 - r_3$	2 : $q_2 = -r_1 - r_3$	3 : $q_3 = -r_1 - r_2$
4 : $u_1 = -v_1 - v_2$	5 : $u_2 = -v_3 - v_4$	6 : $u_3 = -v_5 - v_6$
7 : $q_1 = 2q_2 + 2r_1$	8 : $u_1/t_1 = u_2/t_2 = u_3/t_3 = K_s(q_i/s_i)^{\frac{1}{2}}$	9 : $u_1/t_1 = u_2/t_2 = u_3/t_3 = -2K_s(q_i/s_i)^{\frac{1}{2}}$

10 : $q_1/s_1 = q_2/s_2 = q_3/s_3$ 11 : $r_1/s_1 = r_2/s_2 = r_3/s_3 = q_1/(s_2 + s_3) = q_2/(s_1 + s_3) = q_3/(s_1 + s_2)$

12 : $u_1/v_1 = u_2/v_3 = u_3/v_5$ 13 : $r_i \leq 0$

The factors K_s, in the above relations No. 8 and 9, are equal to $+1$ or -1, and are determined by the sign of the product of the Raman tensor elements : $a'b'$ in the representative modes C_3:A or D_3:A_1, and $h'g'$ or $d'e'$ in the representative mode D_3:E.

---

this defect is available with a different BT. In this simple example the second mode can only be a $C_2[110]$:B mode, and correspondingly the defect must possess the representative symmetry $C_2[110]$.

In addition to the set of IP relations of one mode, which determine the BT, for some defect symmetries O_1 relations are available between the IP's of different modes of the same defect. These IP relations, which are given in Table IX, are based on the population numbers, which are common for the different modes. They make it possible,

e.g., to distinguish the modes of $D_2[110]$ from the other modes in the set given by (19b) and (19c) provided that several modes belonging to the same defect are measured. In favorable circumstances all 25 representative modes can be distinguished by a multimode analysis except for the C_1:A mode.

E. Observed versus the actual behavior type

The BT which we have been discussing so far is what we will call the *actual* BT: Its characteristic IP relations

TABLE VIII. BT of the Raman IP's are given for each symmetry F_1 of the orientating operator $\hat{F}$ and for each representative dynamical mode. The relations which determine these BT's are given in Table VII. The maximum number N_{dis} of the representative modes which can be distinguished is also given for each of the F_1. The modes are numbered as in Table VI.

O_1		Mode	$F_1=$	C_1	$C_2[100]$	$C_2[011]$	$D_2[100]$	$D_2[011]$	$C_3[111]$	$D_3[111]$	$C_4[100]$	$D_4[100]$	T
C_1	1	A		1	16	25	37	41	46	55	56	58	60
$C_2[010]$	2	A		2	17	26	37	42	47	51	56	58	60
	3	B		3	18	27	6	43	48	48	30	30	15
$C_2[110]$	4	A		1	16	25	37	41	46	55	56	58	60
	5	B		4	19	28	38a	44	49	53a	57a	45a	40
$D_2[100]$	6	A		5	5	29	5	29	50	50	29	29	50
	7	B_1		6	6	30	6	30	15	15	30	30	15
$D_2[110]$	8	A		7	20	31	37	42	51	51	58	58	60
	9	B_1		8	8	32	8	32	14	14	32	32	14
	10	B_2		3	18	27	6	43	48	48	30	30	15
	11	B_3		3	18	27	6	43	48	48	30	30	15
$C_3[111]$	12	A		9	21	33	39	21	52	52	39	39	39
	13	E		10	22	34	40	23a	49	53a	59	40	40
$D_3[111]$	14	A_1		9	21	33	39	21	52	52	39	39	39
	15	E		11	23b	35	40	23b	53b	53b	40	40	40
$C_4[001]$	16	A		5	5	29	5	29	50	50	29	29	50
	17	B		12	24	36	38b	45b	54	40	57b	45b	40
	18	E		6	6	30	6	30	15	15	30	30	15
$D_4[001]$	19	A_1		5	5	29	5	29	50	50	29	29	50
	20	B_1		8	8	32	8	32	14	14	32	32	14
	21	B_2		6	6	30	6	30	15	15	30	30	15
	22	E		6	6	30	6	30	15	15	30	30	15
T	23	A		13	13	13	13	13	13	13	13	13	13
	24	E		14	14	14	14	14	14	14	14	14	14
	25	T		15	15	15	15	15	15	15	15	15	15
N_{dis}				15	15	15	11	14	12	11	13	11	7

are the ones required by the actual symmetry of the defect and the orientating operator $\hat{F}$. The BT which is distilled from the experimental data is called the *observed* BT: It can accidentally possess IP relations which are not implied by the symmetry of the defect. For instance, a C_{3v}:A_1 mode with $F_1=T$ does not require $q=0$ or $q=s$ (Tables VII and VIII), but if the diagonal elements of the Raman tensor would happen to be near zero or to be near the value of the off-diagonal elements, one would observe one of the above IP relations if the experimental intensities could not be measured with sufficient precision. However, the symmetry-required IP relations can never be broken: For instance, if an actual BT possesses a IP relation such as $x=0$ or $x_1=x_2$ it is impossible to observe $x\neq0$ or $x_1\neq x_2$ given an adequate statistical data processing.

The accidental additional IP relations can make the observed BT different from the actual BT for a given center. This complication should be kept in mind when performing a BT analysis. Therefore, we have listed in Table X all the possible actual BT's corresponding to a given observed BT. This hierarchy can be expressed by saying that

the observed BT may possess a higher symmetry than the actual BT.

F. Other possible analysis methods

Independent information about the model of the defect or about the relative values of the population numbers N_n is very helpful in the BT analysis. The population numbers can sometimes be estimated from other experiments, e.g., from polarized optical absorption or electron spin resonance. A hypothetical model may permit one in eliminating some of the possible defect symmetries and in predicting the effect of the preferential orientation process. From such data additional constraints on the IP can often be derived, such as their sign or their relative magnitudes, and eventually some of the possible representative modes can be eliminated narrowing down the choice.

The combination of Raman measurements with external data permits one in some cases to distinguish between dynamical modes which were classified in the same representative mode (Table VI): The B_1, B_2, and B_3 modes in $D_2[100]$ defect symmetry can be distinguished if

TABLE IX. Relations which exist between the Raman IP's of the representative dynamical modes (identified by the numbers given in Table VI) belonging to the same defect, and which can be measured in the same Raman experiment. If equalities among the IP's exist, as given by the BT (Tables VII and VIII), they can be substituted into these relations. This often permits one to apply the relations even when only part of the IP are available from the experiments.

Defect symmetry O_1	Representative modes	The IP relations between different modes of the same defect
$C_2[010]$	2,3	$(u_1/u_2)_A = (t_1/t_2)_B = (N_5 - N_6 + N_{21} - N_{22})/(N_1 - N_2 + N_{13} - N_{14})$
	2,3	$(u_1/u_3)_A = (t_1/t_3)_B = (N_5 - N_6 + N_{21} - N_{22})/(N_9 - N_{11} + N_{17} - N_{19})$
	2,3	$(u_2/u_3)_A = (t_2/t_3)_B = (N_1 - N_2 + N_{13} - N_{14})/(N_9 - N_{11} + N_{17} - N_{19})$
$D_2[110]$	8,9	$(s_1/s_2)_A = (r_1/r_2)_{B_1} = (N_{13} + N_{14})/(N_9 + N_{10})$
	8,9	$(s_1/s_3)_A = (r_1/r_3)_{B_1} = (N_{13} + N_{14})/(N_1 + N_3)$
	8,9	$(s_2/s_3)_A = (r_2/r_3)_{B_1} = (N_9 + N_{10})/(N_1 + N_3)$
	8,10,11	$(u_1/u_2)_A = (v_1/v_3)_A = (t_1/t_2)_{B_2} = (t_1/t_2)_{B_3} = (N_{13} - N_{14})/(N_9 - N_{10})$
	8,10,11	$(u_1/u_3)_A = (v_1/v_5)_A = (t_1/t_3)_{B_2} = (t_1/t_3)_{B_3} = (N_{13} - N_{14})/(N_1 - N_3)$
	8,10,11	$(u_2/u_3)_A = (v_3/v_5)_A = (t_2/t_3)_{B_2} = (t_2/t_3)_{B_3} = (N_9 - N_{10})/(N_1 - N_3)$
	8,9,10,11	$[(s_2 + s_3)/(s_1 + s_3)]_A = (q_1/q_2)_{B_1} = (s_1/s_2)_{B_2} = (s_1/s_2)_{B_3} = \dfrac{(N_1 + N_3 + N_9 + N_{10})}{(N_1 + N_3 + N_{13} + N_{14})}$
	8,9,10,11	$[(s_2 + s_3)/(s_1 + s_2)]_A = (q_1/q_3)_{B_1} = (s_1/s_3)_{B_2} = (s_1/s_3)_{B_3} = \dfrac{(N_1 + N_3 + N_9 + N_{10})}{(N_9 + N_{10} + N_{13} + N_{14})}$
	8,9,10,11	$[(s_1 + s_3)/(s_1 + s_2)]_A = (q_2/q_3)_{B_1} = (s_2/s_3)_{B_2} = (s_2/s_3)_{B_3} = \dfrac{(N_1 + N_3 + N_{13} + N_{14})}{(N_9 + N_{10} + N_{13} + N_{14})}$
	10,11	$(t_i)_{B_2}(t_i)_{B_3} \leq 0$
$C_3[111]$	12,13	$(u_1/u_2)_A = (t_1/t_2)_A = (u_1/u_2)_E = (t_1/t_2)_E = \dfrac{N_1 - N_2 + N_3 - N_4 + N_5 - N_6 + N_7 - N_8}{N_1 - N_2 - N_3 + N_4 + N_5 - N_6 - N_7 + N_8}$
	12,13	$(u_1/u_3)_A = (t_1/t_3)_A = (u_1/u_3)_E = (t_1/t_3)_E = \dfrac{N_1 - N_2 + N_3 - N_4 + N_5 - N_6 + N_7 - N_8}{N_1 + N_2 - N_3 - N_4 + N_5 + N_6 - N_7 - N_8}$
	12,13	$(u_2/u_3)_A = (t_2/t_3)_A = (u_2/u_3)_E = (t_2/t_3)_E = \dfrac{N_1 - N_2 - N_3 + N_4 + N_5 - N_6 - N_7 + N_8}{N_1 + N_2 - N_3 - N_4 + N_5 + N_6 - N_7 - N_8}$
	12,13	$(t_1/s_1)_A = -2(t_1/s_1)_E = \dfrac{N_1 - N_2 + N_3 - N_4 + N_5 - N_6 + N_7 - N_8}{N_1 + N_2 + N_3 + N_4 + N_5 + N_6 + N_7 + N_8}$
	12,13	$(t_2/s_1)_A = -2(t_2/s_1)_E = \dfrac{N_1 - N_2 - N_3 + N_4 + N_5 - N_6 - N_7 + N_8}{N_1 + N_2 + N_3 + N_4 + N_5 + N_6 + N_7 + N_8}$
	12,13	$(t_3/s_1)_A = -2(t_3/s_1)_E = \dfrac{N_1 + N_2 - N_3 - N_4 + N_5 + N_6 - N_7 - N_8}{N_1 + N_2 + N_3 + N_4 + N_5 + N_6 + N_7 + N_8}$
	12,13	$(t_i)_A(t_i)_E \leq 0$
$D_3[111]$	14,15	$(u_1/u_2)_{A_1} = (t_1/t_2)_{A_1} = (u_1/u_2)_E = (t_1/t_2)_E = (N_1 - N_2 + N_3 - N_4)/(N_1 - N_2 - N_3 + N_4)$
	14,15	$(u_1/u_3)_{A_1} = (t_1/t_3)_{A_1} = (u_1/u_3)_E = (t_1/t_3)_E = (N_1 - N_2 + N_3 - N_4)/(N_1 + N_2 - N_3 - N_4)$
	14,15	$(u_2/u_3)_{A_1} = (t_2/t_3)_{A_1} = (u_2/u_3)_E = (t_2/t_3)_E = (N_1 - N_2 - N_3 + N_4)/(N_1 + N_2 - N_3 - N_4)$
	14,15	$(t_1/s_1)_{A_1} = -2(t_1/s_1)_E = (N_1 - N_2 + N_3 - N_4)/(N_1 + N_2 + N_3 + N_4)$
	14,15	$(t_2/s_1)_{A_1} = -2(t_2/s_1)_E = (N_1 - N_2 - N_3 + N_4)/(N_1 + N_2 + N_3 + N_4)$
	14,15	$(t_3/s_1)_{A_1} = -2(t_3/s_1)_E = (N_1 + N_2 - N_3 - N_4)/(N_1 + N_2 + N_3 + N_4)$
	14,15	$(t_i)_{A_1}(t_i)_E \leq 0$
$C_4[100]$	17,18	$(q_1/q_2)_B = (s_1/s_2)_E = (N_1 + N_3 + N_9 + N_{10})/(N_1 + N_3 + N_{13} + N_{14})$
	17,18	$(q_1/q_3)_B = (s_1/s_3)_E = (N_1 + N_3 + N_9 + N_{10})/(N_9 + N_{10} + N_{13} + N_{14})$
	17,18	$(q_2/q_3)_B = (s_2/s_3)_E = (N_1 + N_3 + N_{13} + N_{14})/(N_9 + N_{10} + N_{13} + N_{14})$
$D_4[100]$	20,21	$(r_1/r_2)_{B_1} = (s_1/s_2)_{B_2} = N_{13}/N_9$
	20,21	$(r_1/r_3)_{B_1} = (s_1/s_3)_{B_2} = N_{13}/N_1$
	20,21	$(r_2/r_3)_{B_1} = (s_2/s_3)_{B_2} = N_9/N_1$
	20,21,22	$(q_1/q_2)_{B_1} = [(s_2 + s_3)/(s_1 + s_3)]_{B_2} = (s_1/s_2)_E = (N_1 + N_9)/(N_1 + N_{13})$
	20,21,22	$(q_1/q_3)_{B_1} = [(s_2 + s_3)/(s_1 + s_2)]_{B_2} = (s_1/s_3)_E = (N_1 + N_9)/(N_9 + N_{13})$
	20,21,22	$(q_2/q_3)_{B_1} = [(s_1 + s_3)/(s_1 + s_2)]_{B_2} = (s_2/s_3)_E = (N_1 + N_{13})/(N_9 + N_{13})$

independent information about the population numbers N_n is available.

III. APPLICATION OF BEHAVIOR-TYPE THEORY TO PRACTICAL EXPERIMENTS

A. Nature and symmetry properties of the orientating operator $\hat{F}$

In the foregoing treatment we have described the process of preferential reorientation or destruction of point defects by an orientating operator $\hat{F}$, acting on the population numbers N_n (see Secs. II B and II C). In principle this operator could represent any physical process which alters the population numbers. Polarized optical excitation in an absorption band of the defect is often a convenient method. The excitation may destroy the point defect preferentially in specific orientations, or it may reorient the defects preferentially. In the following we mainly concentrate on this optical method of preferential bleaching and reorientation.

For virtually all defects the optical transition employed

TABLE X. *Observed* BT's are given together with the corresponding *actual* BT (see Sec. II E). Only those actual BT's must be considered which can occur for the symmetry F_1 employed in the experiment (Table VIII). The BT No. 15 can reduce to nearly any other BT, and only the actual BT's which can never correspond to this observed BT are listed between parentheses.

Observed BT	Possible actual BT	Observed BT	Possible actual BT
1	1	2	1 2
3	1 3 4	4	1 4
5	1 2 5 7 16 17 20 37	6	1 2 3 4 6 7 12 16 17 18 19 20 24 37 38a 38b
7	1 2 7	8	1 2 4 5 7 8 12 16 17 19 20 24 37 38a 38b
9	1 9	10	1 10
11	1 11	12	1 2 12
13	1 2 5 7 9 13 16 17 20 21 25 26 29 31 33 37 39 41 42 46 47 50 51 52 55 56 58 60	14	1 2 5 7 10 11 14 16 17 20 22 23a 23b 25 26 29 31 34 35 37 40 41 42 46 47 49 50 51 53a 53b 54 55 56 58 59 60
15	(5 8 13 14 29 32 50)	16	16
17	16 17	18	16 18
19	16 19	20	16 17 20
21	16 21 41	22	16 22
23a	16 23a 41	23b	16 23a 23b 41
24	16 17 24	25	25
26	25 26	27	25 27 28
28	25 28	29	25 26 29 31 41 42 56 58
30	25 26 27 28 30 31 36 41 42 43 44 45a 45b 56 57a 57b 58	32	25 26 28 29 31 32 36 41 42 44 45a 45b 56 57a 57b 58
31	25 26 31	33	25 33
34	25 34	35	25 35
36	25 26 36	37	37
38a	37 38a	38b	37 38b
39	37 39 56 58 60	40	37 40 51 53a 55 56 58 59 60
41	41	42	41 42
43	41 43 44	44	41 44
45a	41 42 44 45a 58	45b	41 42 44 45b 58
46	46	47	46 47
48	46 48 49 52 53a 53b 55	49	46 49
50	46 47 50 51 55 60	51	46 47 51 55
52	46 52 55	53a	46 53a 55
53b	46 53a 53b 55	54	46 47 49 54
55	55	56	56
57a	56 57a	57b	56 57b
58	56 58	59	56 59
60	60		

for the preferential orientation possesses pure electric dipole character. As a result the direction of the polarization vector determines the symmetry F_1 of the orientating operator $\widehat{F}$. It is relatively easy to realize experimentally the following symmetries of optical excitation: Unpolarized light incident along [100] or light polarized along this direction yields $F_1 = D_4[100]$. An analogous optical excitation obtained by replacing the propagation or polarization direction by [110] and [111] yields $F_1 = D_2[110]$ and $F_1 = D_3[111]$, respectively. Light with a polarization vector in the (100) plane, but not along $\langle 100 \rangle$ or $\langle 110 \rangle$ directions, results in a symmetry $F_1 = C_2[100]$. Finally, $F_1 = C_2[011]$ is obtained when the polarization vector is lying in the (011) plane, but not along $\langle 110 \rangle$, $\langle 100 \rangle$, or $\langle 110 \rangle$ directions.

In actual experiments it is necessary to consider whether the concentration and the population distribution of the defect over its orientations are both uniform over the whole crystal. The effect of an optical excitation is stronger near the surface of the crystal which has received the irradiation, and is diminishing with increasing distance from this surface. In such a case it is very difficult to rotate the crystal without changing the population numbers N_n which are measured in the Raman experiment.

B. Practical sets of optical polarization geometries

For any given orientating operator $\widehat{F}$ it is in principle possible to determine 21 IP's (see Sec. II A) of a dynamical mode from a set of 21 measurements using well-chosen polarization directions of the incident and scattered light. However, in a practical experiment such an extended set of accurate measurements is often hard to perform. Moreover, the experimental setup often limits the choice of the polarization vectors $\vec{a}$ and $\vec{b}$: We will only consider the perpendicular scattering geometry which is the one commonly applied in Raman experiments. A pair $(\vec{a}, \vec{b})$ will further be called an optical geometry pair (OGP). It is useful to choose the OGP in such a way that the expressions of the scattered intensities as a function of the IP [Eqs. (7)] are as simple as possible, and still permit one in the determination of the highest number of IP's in as few measurements as possible. Finally, the different intensity measurements must be performed in the same experimental conditions in order to obtain the same experimental efficiency factor k [Eq. (1)]. This factor is influenced by the orientation of the sample, the condition of the crystal surfaces, the position of the laser beam, and so on. Three OGP sets were selected on the basis of the criteria given above (Table XI and Fig. 2). The OGP sets are further di-
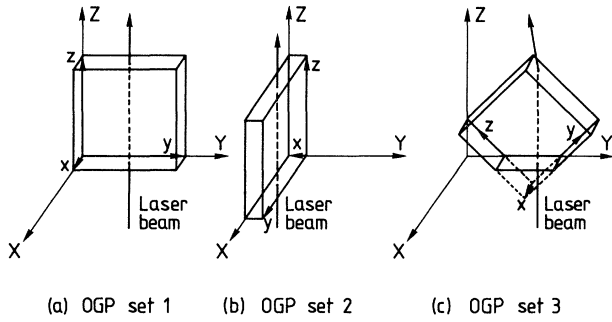
TABLE XI. Explicit expressions of the Raman intensities $I_{\alpha,\beta}$ as a function of the Raman IP's for each of the practical OGP's discussed in Sec. III B. The right part of the table lists the error orders of the angular dependence of these intensities (see Sec. III E) for each symmetry F_1 of the orientating operator $\hat{F}$. Each set of OGP is divided in several subsets which are often measured together in the experiments.

OGP	Raman intensity expression	C$_1$	C$_2$[100]	C$_2$[011]	D$_2$[100]	D$_2$[011]	C$_3$	D$_3$	C$_4$	D$_4$	T
set 1.1	$I_{x,y} = s_3$	1	1	1	2	1	1	1	2	2	2
	$I_{x,z} = s_2$	1	1	1	2	1	1	1	2	2	2
	$I_{y,z} = s_1$	1	1	1	2	2	1	1	1	2	2
	$I_{y,y} = q_2$	1	1	1	2	1	1	1	1	2	2
set 1.2	$I_{y,yz} = \frac{1}{2}(s_1 + q_2 + 2v_1)$	1	1	1	1	1	1	1	1	1	1
	$I_{y,y\bar{z}} = \frac{1}{2}(s_1 + q_2 - 2v_1)$	1	1	1	1	1	1	1	1	1	1
	$I_{x,y\bar{z}} = \frac{1}{2}(s_2 + s_3 - 2t_1)$	1	1	1	1	2	1	1	2	2	2
	$I_{x,yz} = \frac{1}{2}(s_2 + s_3 + 2t_1)$	1	1	1	1	2	1	1	2	2	2
set 1.3	$I_{xy,y} = \frac{1}{2}(q_2 + s_3 + 2v_6)$	1	1	1	1	1	1	1	1	1	1
	$I_{x\bar{y},y} = \frac{1}{2}(q_2 + s_3 - 2v_6)$	1	1	1	1	1	1	1	1	1	1
	$I_{xy,z} = \frac{1}{2}(s_1 + s_2 + 2t_3)$	1	1	1	1	1	1	1	1	1	2
	$I_{x\bar{y},z} = \frac{1}{2}(s_1 + s_2 - 2t_3)$	1	1	1	1	1	1	1	1	1	2
set 1.4	$I_{xy,yz} = \frac{1}{4}(q_2 + s_1 + s_2 + s_3) + \frac{1}{2}(t_1 + t_2 + t_3 + u_2 + v_1 + v_6)$	1	1	1	1	1	1	1	1	1	1
	$I_{xy,y\bar{z}} = \frac{1}{4}(q_2 + s_1 + s_2 + s_3) + \frac{1}{2}(-t_1 - t_2 + t_3 - u_2 - v_1 + v_6)$	1	1	1	1	1	1	1	1	1	1
	$I_{x\bar{y},yz} = \frac{1}{4}(q_2 + s_1 + s_2 + s_3) + \frac{1}{2}(t_1 - t_2 - t_3 - u_2 + v_1 - v_6)$	1	1	1	1	1	1	1	1	1	1
	$I_{x\bar{y},y\bar{z}} = \frac{1}{4}(q_2 + s_1 + s_2 + s_3) + \frac{1}{2}(-t_1 + t_2 - t_3 + u_2 - v_1 - v_6)$	1	1	1	1	1	1	1	1	1	1
set 2.1	$I_{x,x} = q_1$	1	2	1	2	2	1	1	2	2	2
	$I_{x,z} = s_2$	1	1	1	2	1	1	1	2	2	2
	$I_{y,z} = s_1$	1	1	1	2	2	1	1	1	2	2
	$I_{y,x} = s_3$	1	1	1	2	1	1	1	2	2	2
set 2.2	$I_{y,xz} = \frac{1}{2}(s_1 + s_3 + 2t_2)$	1	1	1	1	1	1	1	1	1	2
	$I_{y,x\bar{z}} = \frac{1}{2}(s_1 + s_3 - 2t_2)$	1	1	1	1	1	1	1	1	1	2
	$I_{x,x\bar{z}} = \frac{1}{2}(q_1 + s_2 - 2v_3)$	1	1	1	1	1	1	1	1	1	1
	$I_{x,xz} = \frac{1}{2}(q_1 + s_2 + 2v_3)$	1	1	1	1	1	1	1	1	1	1
set 2.3	$I_{xy,x} = \frac{1}{2}(q_1 + s_3 + 2v_5)$	1	1	1	1	1	1	1	1	1	1
	$I_{x\bar{y},x} = \frac{1}{2}(q_1 + s_3 - 2v_5)$	1	1	1	1	1	1	1	1	1	1
	$I_{xy,z} = \frac{1}{2}(s_1 + s_2 + 2t_3)$	1	1	1	1	1	1	1	1	1	2
	$I_{x\bar{y},z} = \frac{1}{2}(s_1 + s_2 - 2t_3)$	1	1	1	1	1	1	1	1	1	2
set 2.4	$I_{xy,xz} = \frac{1}{4}(q_1 + s_1 + s_2 + s_3) + \frac{1}{2}(t_1 + t_2 + t_3 + u_1 + v_3 + v_5)$	1	1	1	1	1	1	1	1	1	1
	$I_{xy,x\bar{z}} = \frac{1}{4}(q_1 + s_1 + s_2 + s_3) + \frac{1}{2}(-t_1 - t_2 + t_3 - u_1 - v_3 + v_5)$	1	1	1	1	1	1	1	1	1	1
	$I_{x\bar{y},xz} = \frac{1}{4}(q_1 + s_1 + s_2 + s_3) + \frac{1}{2}(-t_1 + t_2 - t_3 - u_1 + v_3 - v_5)$	1	1	1	1	1	1	1	1	1	1
	$I_{x\bar{y},x\bar{z}} = \frac{1}{4}(q_1 + s_1 + s_2 + s_3) + \frac{1}{2}(t_1 - t_2 - t_3 + u_1 - v_3 - v_5)$	1	1	1	1	1	1	1	1	1	1
set 3.1	$I_{x,y} = s_3$	1	1	1	2	1	1	1	2	2	2
	$I_{x,z} = s_2$	1	1	1	2	1	1	1	2	2	2
	$I_{y\bar{z},z} = \frac{1}{2}(q_3 + s_1 - 2v_2)$	1	1	1	1	1	1	1	1	1	1
	$I_{y\bar{z},y} = \frac{1}{2}(q_2 + s_1 - 2v_1)$	1	1	1	1	1	1	1	1	1	1
set 3.2	$I_{x,yz} = \frac{1}{2}(s_2 + s_3 + 2t_1)$	1	1	1	1	2	1	1	2	2	2
	$I_{x,y\bar{z}} = \frac{1}{2}(s_2 + s_3 - 2t_1)$	1	1	1	1	2	1	1	2	2	2
	$I_{y\bar{z},y\bar{z}} = \frac{1}{4}(q_2 + q_3) + \frac{1}{2}r_1 + s_1 - v_1 - v_2$	1	2	1	2	2	1	2	2	2	2
	$I_{y\bar{z},yz} = \frac{1}{4}(q_2 + q_3) - \frac{1}{2}r_1$	1	1	1	2	2	1	1	1	2	2
set 3.3	$I_{x(y\bar{z}),z} = \frac{1}{4}(q_3 + s_1) + \frac{1}{2}(s_2 + \sqrt{2}t_3 - v_2 - \sqrt{2}v_4)$	1	1	1	1	1	1	1	1	1	1
	$I_{\bar{x}(y\bar{z}),z} = \frac{1}{4}(q_3 + s_1) + \frac{1}{2}(s_2 - \sqrt{2}t_3 - v_2 + \sqrt{2}v_4)$	1	1	1	1	1	1	1	1	1	1
	$I_{x(y\bar{z}),y} = \frac{1}{4}(q_2 + s_1) + \frac{1}{2}(s_3 - \sqrt{2}t_2 - v_1 + \sqrt{2}v_6)$	1	1	1	1	1	1	1	1	1	1
	$I_{\bar{x}(y\bar{z}),y} = \frac{1}{4}(q_2 + s_1) + \frac{1}{2}(s_3 + \sqrt{2}t_2 - v_1 - \sqrt{2}v_6)$	1	1	1	1	1	1	1	1	1	1
set 3.4	$I_{x(y\bar{z}),yz} = \frac{1}{8}(q_2 + q_3) + \frac{1}{4}(s_2 + s_3 - r_1) + \frac{1}{2}(t_1 + v_6) + \frac{\sqrt{2}}{4}(u_2 - u_3 - v_4)$	1	1	1	1	1	1	1	1	1	1
	$I_{\bar{x}(y\bar{z}),yz} = \frac{1}{8}(q_2 + q_3) + \frac{1}{4}(s_2 + s_3 - r_1) + \frac{1}{2}(t_1 - v_6) + \frac{\sqrt{2}}{4}(-u_2 + u_3 + v_4)$	1	1	1	1	1	1	1	1	1	1
	$I_{x(y\bar{z}),y\bar{z}} = \frac{1}{8}(q_2 + q_3) + \frac{1}{4}(s_2 + s_3 + r_1) + \frac{1}{2}(s_1 - t_1 - v_1 - v_2) + \frac{\sqrt{2}}{4}(-u_2 + u_3 - v_4 + v_6) + \frac{\sqrt{2}}{2}(-t_2 + t_3)$	1	1	1	1	1	1	1	1	1	1
	$I_{\bar{x}(y\bar{z}),y\bar{z}} = \frac{1}{8}(q_2 + q_3) + \frac{1}{4}(s_2 + s_3 + r_1) + \frac{1}{2}(s_1 - t_1 - v_1 - v_2) + \frac{\sqrt{2}}{4}(u_2 - u_3 + u_4 - v_6) + \frac{\sqrt{2}}{2}(t_2 - t_3)$	1	1	1	1	1	1	1	1	1	1

(a) OGP set 1   (b) OGP set 2   (c) OGP set 3

FIG. 2. Schematic representation of the optical geometries for OGP sets 1, 2, and 3. The laboratory and crystal reference frames are denoted by (X, Y, Z) and (x, y, z), respectively. The scattered light is in each case collected along X. The crystal faces are $\{100\}$ planes except in OGP set 3 where there is an additional face along a $\{110\}$ plane.

vided into subsets which are often measured together in the experiments. The pairs $(\vec{a}_i, \vec{b}_i)$ within a set can be realized without rotating the sample. For this reason the same factor k will occur in experiments belonging to the same set, if all other experimental conditions are kept constant.

In Table XI the experimentally measured intensities $I_{\alpha,\beta}$ are given as a function of the IP. The notation introduced for the rotation axes (Sec. II A) is also employed for the polarization directions α and β, which are expressed in the x, y, and z axes fixed to the principal $\langle 100 \rangle$ crystal directions. For example, $\alpha = x\bar{y}$ means $\alpha || [1\bar{1}0]$, while $\alpha = x(yz)$ stands for a polarization vector α in the $(01\bar{1})$ plane at 45° between [100] and [011].

From the Raman intensities measured in one or even several OGP sets it is not possible to determine all of the IP's of a dynamical mode. Only part of the IP's occurs in each set of intensity equations (Table XI). Moreover, some of the IP's cannot be solved from these equations. In Table XII the inverse expressions are given for the IP's

TABLE XII. Raman IP's which can be solved from the expressions in Table XI for each set of OGP's separately, and without taking into account the relations between the IP's which result from the symmetry F_1 of the orientating operator $\hat{F}$. Also included are some simple IP combinations which are useful in a BT analysis using several OGP sets (Sec. III B).

Optical geometry	IP expression
set 1	$q_2 = I_{y,y}$ $s_1 = I_{y,z}$ $s_2 = I_{x,z}$ $s_3 = I_{x,y}$ $t_1 = \frac{1}{2}(I_{x,yz} - I_{x,y\bar{z}})$ $t_3 = \frac{1}{2}(I_{xy,z} - I_{x\bar{y},z})$ $v_1 = \frac{1}{2}(I_{y,yz} - I_{y,y\bar{z}})$ $v_6 = \frac{1}{2}(I_{xy,y} - I_{x\bar{y},y})$ $t_2 + u_2 = \frac{1}{2}(I_{xy,yz} - I_{xy,y\bar{z}} - I_{x\bar{y},yz} + I_{x\bar{y},y\bar{z}})$
set 2	$q_1 = I_{x,x}$ $s_1 = I_{y,z}$ $s_2 = I_{x,z}$ $s_3 = I_{x,y}$ $t_2 = \frac{1}{2}(I_{y,xz} - I_{y,x\bar{z}})$ $t_3 = \frac{1}{2}(I_{xy,x} - I_{x\bar{y},x})$ $v_3 = \frac{1}{2}(I_{x,xz} - I_{x,x\bar{z}})$ $v_5 = \frac{1}{2}(I_{xy,x} - I_{x\bar{y},x})$ $u_1 + t_1 = \frac{1}{2}(I_{xy,xz} - I_{xy,x\bar{z}} - I_{x\bar{y},xz} + I_{x\bar{y},x\bar{z}})$
set 3	$s_2 = I_{x,z}$ $s_3 = I_{x,y}$ $t_1 = \frac{1}{2}(I_{x,yz} - I_{x,y\bar{z}})$ $t_3 - v_4 = \frac{\sqrt{2}}{2}(I_{x(y\bar{z}),z} - I_{\bar{x}(y\bar{z}),z})$ $v_6 - t_2 = \frac{\sqrt{2}}{2}(I_{x(y\bar{z}),y} - I_{\bar{x}(y\bar{z}),y})$ $u_2 - u_3 - v_4 + \sqrt{2}v_6 = \sqrt{2}(I_{x(y\bar{z}),y\bar{z}} - I_{\bar{x}(y\bar{z}),y\bar{z}})$

and for relatively simple linear combinations of the IP's, which can be calculated from experiments in each OGP set separately. These inverse expressions were solved from the equations in Table XI for a general symmetry F_1. For a specific symmetry F_1 the IP's must follow at least the minimum BT for the defect symmetry $O_1 = C_1$ (see Sec. II B). The equations of the Raman intensities $I_{\alpha,\beta}$ (Table XI) can be simplified using the relations included in this minimum BT (Sec. II D 2) for the symmetry F_1. As a result a higher percentage of the often less numerous independent IP's can be determined. For example, for $F_1 = T$ and OGP set 3 the three independent parameters q, r, and s can all be determined (BT no. 60 and equations in Table XI). The number of available independent IP's is listed in Table XIII(a) and compared with the maximum number of independent IP's for each of the symmetries F_1.

In favorable experimental circumstances it is possible to combine the measurements in different OGP sets in order to determine an even large number of IP's. Even if the symmetry of $\hat{F}$ is not taken into account in order to simplify the expressions for $I_{\alpha,\beta}$, the combination of the three OGP sets yields 16 IP's out of the full set of 21 IP's. Such a combined determination is possible if one can obtain identical experimental conditions for different orientations of the crystal, and as a result the same k factor occurs. In other cases, it is possible to determine the ratio between the k factors because the same polarization OGP occurs in the different sets. For example, $I_{x,z}$ can be measured in each of the three sets. All of the measurements must, however, relate to the same population distribution of the defect over its possible orientations.

C. Behavior-type analysis with a limited number of IP's

When only part of the IP can be determined from the experiment, either from measurements in a single OGP set or by combined measurements in several sets, it is possible to check only part of the relations which define the BT [Eqs. (18), Table VII]. As a result it will sometimes not be possible to distinguish between different BT's for a given F_1, and in general fewer representative modes can be distinguished. For each symmetry F_1 we have determined the representative modes which cannot be distinguished on the basis of this limited BT analysis: They are given between parentheses in Table XIII(b). Each of the OGP sets is considered, as well as useful combinations of several sets. In general the number of modes which can be distinguished, N_{dis} [see Table XIII(b)], is lower than 15, the maximum value for a BT analysis, except for an analysis of measurements in the three OGP sets, taking $F_1 = C_2[011]$. The latter, however, is a quite difficult experiment.

As mentioned before in Sec. II D 2 only one of the different symmetry groups, F_1, which can be transformed into each other by a rotation $\hat{R}_n \in O$, has been considered in our calculations. The BT resulting from a rotated symmetry F_1 of the orientating operator $\hat{F}$ can be obtained from the BT before rotation by a permutation of the IP. If a full set of 21 IP's is available the representative modes

which can or cannot be distinguished from one another are the same for different rotated groups F_1. However, this is not true when only part of the IP can be determined, as is often the case in experiments employing one or several of the OGP sets. In this case the equations in Table XI must be considered together with the suitable permutations of the IP in the BT (Table VII) in order to obtain the modified Table XIII(b). The orientations of the groups F_1 which were discussed throughout this paper and which are listed in Table XIII were chosen because they offer the best opportunities for applying the BT analysis in combination with the chosen OGP.

It is often very fruitful to combine two or more experiments in which different symmetries F_1 of the orientating operator $\hat{F}$ and, eventually, different OGP sets, are employed. In this case the population numbers N_n are different, and different sets of IP's result. However, for each of the symmetries F_1 the possible BT and the corresponding possible representative modes can be determined (Tables VIII and VII). Only those modes are selected which are compatible with the results of all of the experiments with different F_1. For example, from the BT analysis on the basis of an experiment with $F_1 = D_2[011]$ and an OGP set 1 only ten sets of representative modes can be distinguished, i.e., $N_{dis} = 10$ [Table XIII(b)]. For $F_1 = T$ and set 3, one finds $N_{dis} = 7$. If one combines the results of the two experiments, up to 13 sets of modes can be distinguished, compared to the maximum of 15 sets for a BT analysis with a full set of 21 IP values. Moreover, this combined experiment is relatively easy to perform. One can easily derive the effect of similar combinations on the basis of Table XIII(b).

A suitable F_1 and a suitable OGP set can be chosen on the basis of the results in Table XIII(b). For example, if one wants to decide between the modes $C_3:E$, $D_3:E$, $C_4:B$, and $T:T$, which possess the mode numbers 13, 15, 17, and 25 (see Table VIII), respectively, an experiment with $F_1 = D_2[011]$ in OGP set 1 is sufficient. However, to distinguish C_1 from $C_2[110]:B$ and $C_3[111]:E$ with numbers 1, 5, and 13, respectively, is not possible with a single F_1 and a single OGP set: The combination of the BT analysis for $F_1 = D_2[011]$ with set 1 and $F_1 = T$ with set 3, as described in the last paragraph, happens to be a favorable choice.

D. Calculation of the Raman-tensor elements

If for a given defect the representative modes have been determined or if the choice has been narrowed down it may be worthwhile to attempt to solve Eqs. (9) in order to calculate the relative values of the Raman tensors and of the population numbers. The number of independent IP's can be derived from Table VII, and the number of independent population numbers are found from the sets $S_r = F_1 R_n O_1$ (see Sec. II C) and can be obtained from Tables IV(a) and IV(b). The Raman tensors for the modes corresponding to a given representative mode are explicitly given in Table V. Equations (9) or the explicit equations in Table III are simplified by these expressions of the population numbers and the Raman tensors. If the number of independent IP's determined in the experiment is

TABLE XIII. (a) Number of independent Raman IP's μ_{IP} which can be determined from measurements in one set of OGP's or from a combined experiment in several OGP sets, for each symmetry F_1 of the orientating operator $\hat{F}$. When only one or two IP's are not available these are given between parentheses. The cases where the full set of IP's is available are denoted in italic. (b) The sets of representative modes (Table VI) which cannot be distinguished from each other on the basis of the Raman measurements of a single dynamical mode are given for any set of OGP's or a combination of several of them, and for any symmetry F_1 of the orientating operator $\hat{F}$. The maximum number of modes which can be distinguished, $N_{\rm dis}$, is also listed.

(a)

F_1	μ_{IP}	set 1	set 2	set 3	Optical geometry set 1+2	set 1+3	set 1+2+3
C_1	21	8	8	3	14	12	16
$C_2[100]$	13	6	4	3	8	6	8
$C_2[011]$	13	8	5	2	$11(r_1,r_2)$	9	$12(r_2)$
$D_2[100]$	9	4	4	2	5	6	$7(r_2,r_3)$
$D_2[011]$	9	5	3	2	$7(r_1,r_2)$	6	$8(r_2)$
$C_3[111]$	7	$6(r)$	$6(r)$	$6(u)$	$6(r)$	7	7
$D_3[111]$	6	$5(r)$	$5(r)$	$5(u)$	$5(r)$	6	6
$C_4[100]$	7	4	3	1	$5(r_1,r_2)$	$5(q_1,r_2)$	$6(r_2)$
$D_4[100]$	6	3	3	1	$4(r_1,r_2)$	$4(q_1,r_2)$	$5(r_2)$
T	3	$2(r)$	$2(r)$	3	$2(r)$	3	3

(b)

OGP	F_1 symmetry	N_{dis}	Distinguishable sets of representative modes
set 1	$C_1,C_2[100]$	9	(1 4 5) (2 8 17) (3 10 11) (6 9 16 19 20 23 24) (7 18 21 22) (12 14) (13) (15) (25)
	$C_2[011],D_2[011]$	10	(1 4 5) (2 8) (3 10 11) (6 9 16 19 20 23 24) (7 18 21 22) (12 14) (13) (15) (17) (25)
	$D_2[100],D_4$	5	(1 2 4 5 8 17) (3 7 10 11 18 21 22) (6 9 16 19 20 23 24) (12 13 14 15) (25)
	C_4	7	(1 2 4 5 17) (3 7 10 11 18 21 22) (6 9 16 19 20 23 24) (8) (12 14 15) (13) (25)
set 1 or set 2 or set 1+2	C_3	10	(1 4) (2) (3 10 11) (5 13) (6 9 16 19 20 23 24) (7 18 21 22 25) (8) (12 14) (15) (17)
	D_3	9	(1 4) (2 8) (3 10 11) (5 13) (6 9 16 19 20 23 24) (7 18 21 22 25) (12 14) (15) (17)
	T	3	(1 2 3 4 5 8 12 13 14 15 17) (3 7 10 11 18 21 22 25) (6 9 16 19 20 23 24)
set 2	$C_1,C_2[011]$	9	(1 4 5) (2 8 17) (3 10 11) (6 9 16 19 20 23 24) (7 18 21 22) (12 14) (13) (15) (25)
	$C_2[100],D_2{}^a,C_4,D_4$	5	(1 2 4 5 8 17) (3 7 10 11 18 21 22) (6 9 16 19 20 23 24) (12 13 14 15) (25)
set 3	$C_1,C_2[100]$	5	(1 3 4 5 10 11) (2 7 8 17 18 21 22) (6 9 16 19 20 23 24) (12 13 14 15) (25)
	$C_2[011],D_2[011]$	3	(1 3 4 5 10 11 12 13 14 15) (2 7 8 17 18 21 22 25) (6 9 16 19 20 23 24)
	$D_2[100]$	3	(1 2 3 4 5 7 8 10 11 17 18 21 22) (6 9 16 19 20 23 24) (12 13 14 15 25)
	C_4,D_4	2	(1 2 3 4 5 7 8 10 11 12 13 14 15 17 18 21 22 25) (6 9 16 19 20 23 24)
set 3 or set 1+3 or set 1+2+3	C_3	12	(1 4) (2) (3 10 11) (5 13) (6 16 19) (7 18 21 22 25) (8) (9 20 24) (12 14) (15) (17) (23)
	D_3	11	(1 4) (2 8) (3 10 11) (5 13) (6 16 19) (7 18 21 22 25) (9 20 24) (12 14) (15) (17) (23)
	T	7	(1 2 4 8) (3 7 10 11 18 21 22 25) (5 13 15 17) (6 16 19) (9 20 24) (12 14) (23)
set 1+2	$C_1,C_2[011]$	13	(1 4) (2) (3 10 11) (5) (6 9 16 19 20) (7 18 21 22) (8) (12 14) (13) (15) (17) (23 24) (25)
	$C_2[100],D_2[011]$	12	(1 4) (2 8) (3 10 11) (5) (6 9 16 19 20) (7 18 21 22) (12 14) (13) (15) (17) (23 24) (25)
	$D_2[100],D_4$	8	(1 2 4 8) (3 7 10 11 18 21 22) (5) (6 9 16 19 20) (12 13 14 15) (17) (23 24) (25)
	C_4	10	(1 2 4) (3 7 10 11 18 21 22) (5) (6 9 16 19 20) (8) (12 14 15) (17) (13) (23 24) (25)
set 1+3	C_1	11	(1 4 5) (2) (3 10 11) (6 9 16 19 20 23 24) (7 18 21 22) (8) (12 14) (13) (15) (17) (25)
	$C_2[100]$	9	(1 4 5) (2 8 17) (3 10 11) (6 9 16 19 20 23 24) (7 18 21 22) (12 14) (13) (15) (25)
	$C_2[011],D_2[011]$	12	(1 4 5) (2 8) (3 10 11) (6 9 16 19 20) (7 18 21 22) (12 14) (13) (15) (17) (23) (24) (25)
	$D_2[100],D_4$	9	(1 2 4 5 8) (3 7 10 11 18 21 22) (6 9 16 19 20) (12 14) (13 15) (17) (23) (24) (25)
	C_4	11	(1 2 4 5) (3 7 10 11 18 21 22) (6 9 16 19 29) (8) (12 14) (13) (15) (17) (23) (24) (25)
set 1+2+3	C_1	13	(1 4) (2) (3 10 11) (5) (6 9 16 19 20) (7 18 21 22) (8) (12 14) (13) (15) (17) (23 24) (25)
	$C_2[100]$	12	(1 4) (2 8) (3 10 11) (5) (6 9 16 19 20) (7 18 21 22) (12 14) (13) (15) (17) (23 24) (25)
	$C_2[011]$	15	(1 4) (2) (3 10 11) (5) (6 16 19) (7 18 21 22) (8) (9 20) (12 14) (13) (15) (17) (23) (24) (25)
	$D_2[100]$	10	(1 2 4 8) (3 7 10 11 18 21 22) (5) (6 9 16 19 20) (12 14) (13 15) (17) (23) (24) (25)
	$D_2[011]$	14	(1 4) (2 8) (3 10 11) (5) (6 16 19) (7 18 21 22) (9 20) (12 14) (13) (15) (17) (23) (24) (25)
	C_4	13	(1 2 4) (3 7 10 11 18 21 22) (5) (6 16 19) (8) (9 20) (12 14) (13) (15) (17) (23) (24) (25)
	D_4	11	(1 2 4 8) (3 7 10 11 18 21 22) (5) (6 16 19) (9 20) (12 14) (13 15) (17) (23) (24) (25)

^{a}The representative modes $D_2[100]$ and $D_2[011]$ are both included.

higher than the number of unknowns occurring in the equations it is possible to determine part or all of them. Several of the 25 representative modes [Eqs. (19a) and (19c)] which could not be distinguished on the basis of a BT analysis can eventually be identified by this procedure.

E. Experimental errors related to the orientation of the crystal

The main systematic errors which occur in the Raman intensity measurements result from deviation of the crystal orientation with respect to the polarization directions.

In most experimental setups it is, given sufficient care, relatively easy to obtain accurate polarization directions. We have inspected the errors in the Raman measurements ΔI which result from rotations of the sample around the x, y, and z axes, over small angles β_1, β_2, and β_3, respectively. For many of the polarization geometries and symmetries F_1 the angle-dependent intensity errors are of first order, i.e., $\Delta I \sim \beta_i$, but in more favorable cases they are of second order, $\Delta I \sim \beta_i^2$ or $\beta_i \beta_j$; this is indicated in Table XI.

In Table XIV we have listed the leading terms of those Raman intensities which yield first-order angular errors for the symmetry $F_1 = T$ of the orientating operator $\hat{F}$. When the defects are equally distributed over the possible orientations, the relations in Table XIV permit one to test and eventually to correct the orientation of the crystal (see Fig. 2).

IV. RAMAN SCATTERING UNDER THE INFLUENCE OF A SUSTAINED EXTERNAL FIELD

When a sustained external field, e.g., an electric or uniaxial stress field is applied to a crystal in which an anisotropic defect is continually reorientating either through thermal activation or by a tunneling process, changes in the population numbers N_n may be induced. For such cases the present theory is directly applicable. However, if the center is static one may envisage the possibility that the frequency of the dynamical mode under consideration is changed with a different amount for different orientations of the defect. If so, the Raman scattering intensity can be separately measured in different peaks in the Raman spectrum. With minor changes the method presented in this paper can be applied to analyze these types of ex-

TABLE XIV. Explicit expressions of the Raman intensities $I_{\alpha,\beta}$, which possess a first-order angular dependence (Sec. III E and Table XI), without preferential orientation of the defect, $F_1 = T$. These expressions can be applied to monitor and correct the orientation of the crystal.

set 1.2	$I_{y,yz} = \frac{1}{2}(s+q) - (2s+r-q)\beta_1$ $I_{y,y\bar{z}} = \frac{1}{2}(s+q) + (2s+r-q)\beta_1$
set 1.3	$I_{xy,y} = \frac{1}{2}(s+q) + (2s+r-q)\beta_3$ $I_{x\bar{y},y} = \frac{1}{2}(s+q) - (2s+r-q)\beta_3$
set 1.4	$I_{xy,yz} = \frac{1}{4}(3s+q) - \frac{1}{2}(2s+r-q)(\beta_1-\beta_3)$ $I_{xy,y\bar{z}} = \frac{1}{4}(3s+q) + \frac{1}{2}(2s+r-q)(\beta_1+\beta_3)$ $I_{x\bar{y},yz} = \frac{1}{4}(3s+q) - \frac{1}{2}(2s+r-q)(\beta_1+\beta_3)$ $I_{x\bar{y},y\bar{z}} = \frac{1}{4}(3s+q) + \frac{1}{2}(2s+r-q)(\beta_1-\beta_3)$
set 2.2	$I_{x,x\bar{z}} = \frac{1}{2}(s+q) - (2s+r-q)\beta_2$ $I_{x,xz} = \frac{1}{2}(s+q) + (2s+r-q)\beta_2$
set 2.3	$I_{xy,x} = \frac{1}{2}(s+q) - (2s+r-q)\beta_3$ $I_{x\bar{y},x} = \frac{1}{2}(s+q) + (2s+r-q)\beta_3$
set 2.4	$I_{xy,xz} = \frac{1}{4}(3s+q) + \frac{1}{2}(2s+r-q)(\beta_2-\beta_3)$ $I_{xy,x\bar{z}} = \frac{1}{4}(3s+q) - \frac{1}{2}(2s+r-q)(\beta_2+\beta_3)$ $I_{x\bar{y},xz} = \frac{1}{4}(3s+q) + \frac{1}{2}(2s+r-q)(\beta_2+\beta_3)$ $I_{x\bar{y},x\bar{z}} = \frac{1}{4}(3s+q) - \frac{1}{2}(2s+r-q)(\beta_2-\beta_3)$
set 3.1	$I_{y\bar{z},x} = \frac{1}{2}(s+q) - (2s+r-q)\beta_1$ $I_{y\bar{z},y} = \frac{1}{2}(s+q) + (2s+r-q)\beta_1$
set 3.3	$I_{x(y\bar{z}),y} = \frac{1}{4}(3s+q) + \frac{1}{2}(r-q)\beta_1 - \frac{\sqrt{2}}{2}s\beta_2 + \frac{\sqrt{2}}{2}(s+r-q)\beta_3$ $I_{\bar{x}(y\bar{z}),y} = \frac{1}{4}(3s+q) + \frac{1}{2}(r-q)\beta_1 + \frac{\sqrt{2}}{2}s\beta_2 - \frac{\sqrt{2}}{2}(s+r-q)\beta_3$ $I_{x(y\bar{z}),z} = \frac{1}{4}(3s+q) - \frac{1}{2}(r-q)\beta_1 + \frac{\sqrt{2}}{2}(s+r-q)\beta_2 - \frac{\sqrt{2}}{2}s\beta_3$ $I_{\bar{x}(y\bar{z}),z} = \frac{1}{4}(3s+q) - \frac{1}{2}(r-q)\beta_1 - \frac{\sqrt{2}}{2}(s+r-q)\beta_2 + \frac{\sqrt{2}}{2}s\beta_3$
set 3.4	$I_{x(y\bar{z}),yz} = \frac{1}{4}(2s-r+q) + s\beta_1 + \frac{\sqrt{2}}{4}(r-q)(\beta_2+\beta_3)$ $I_{\bar{x}(y\bar{z}),yz} = \frac{1}{4}(2s-r+q) + s\beta_1 - \frac{\sqrt{2}}{4}(r-q)(\beta_2+\beta_3)$ $I_{x(y\bar{z}),y\bar{z}} = \frac{1}{4}(4s+r+q) - \frac{\sqrt{2}}{4}(2s+r+q)(\beta_2+\beta_3)$ $I_{\bar{x}(y\bar{z}),y\bar{z}} = \frac{1}{4}(4s+r+q) + \frac{\sqrt{2}}{4}(2s+r+q)(\beta_2+\beta_3)$

periments. We will assume that even when the external field is applied on the crystal the population numbers N_n of the defect in its possible orientations are equal, $N_n \equiv N$. Furthermore, we will assume that the Raman tensor of the dynamical mode is not perceptibly influenced by the external field. The Raman tensors $\underline{T}^{(n)}$ for the different orientations related by inversion symmetry, v_n and $\hat{i}v_n$, always yield the same Raman scattering intensities. An external field lacking inversion symmetry can possibly yield different frequencies for these two orientations and result in two peaks of equal intensity in the Raman spectrum. Otherwise a double intensity is found in a single Raman peak for these two orientations. By taking this into account, the symmetry properties of the dynamical mode and of the external field can be considered in the cubic point group O instead of O_h in a similar way as discussed for the preferential orientation experiments (see Sec. II A).

If we now consider the subgroup $F_1 \subset O$ as the representative symmetry group of the external field, the orientations of the set V_r corresponding to the right coset F_r of the subgroup F_1 [see Sec. II B, Eqs. (10)] are found to possess the same frequency of the dynamical mode. The Raman scattering intensity is given for each set V_r separately by

$$I^{(r)} = \sum_{v_n \in V_r} I_n ,$$

in which I_n is given by Eq. (2). The intensity expressions [Eqs. (4) and (7)] split up in analogous equations for the intensities $I^{(r)}$, in terms of the partial Raman intensity parameters $P^{(r)}_{iji'j'}$ given by Eq. (11). One can define short notations for these partial IP's analogous to those given in Eqs. (8): $q_i^{(r)}$, $r_i^{(r)}$, $s_i^{(r)}$, $t_i^{(r)}$, $u_i^{(r)}$, and $v_i^{(r)}$. Explicit expressions for these partial IP's can be derived from Table III by setting

$$N_n = \begin{cases} 1, & v_n \in V_r \\ 0, & v_n \notin V_r . \end{cases} \tag{20}$$

It is possible to apply all of the results given in Secs. II and III for the IP's of each Raman peak separately. The BT defined in Table VIII can be strongly simplified by Eqs. (20). For each of the sets V_r a set of equations analogous to Eqs. (9) must be considered, but they all depend on at most five unknowns: the relative values of the Raman tensor elements $T_{ij}^{(1)}$ common to all the possible directions of the defect. As a result solving these equations is much easier for these types of experiments than for the experiments with preferential orientation discussed in Secs. II and III.

V. CONCLUDING REMARKS

In this paper we have systematically investigated the intensities of polarized Raman scattering from point defects in a crystal with a cubic lattice. The partial or complete preferential orientation of the defects allows one to determine to a large extent the symmetry properties of the defect, the nature of the dynamical modes, and sometimes the elements of the Raman tensors. The accompanying tables are helpful in the practical application of this method. It is relatively easy to extend the method to crystals with a different lattice symmetry. It is also possible

to extend the method to resonant scattering by taking into account the antisymmetric nature of the Raman tensor.

We have applied the theory to the study of interstitial hydrogen atom centers in the cubic alkali-halide crystals. The interstitial hydrogen atoms are perturbed by one or two substitutional halogen-ion impurities, heavier than the host halogen ions. Polarized optical bleaching was employed for a partial preferential orientation of the defects. The results are presented in an accompanying paper.[4] They provide a particularly comprehensive example of the practical application of the behavior-type analysis discussed in this paper.

APPENDIX A: PROOF OF EQ. (10b) IN SEC. II B

By definition two rotations $\hat{R}_p$ and $\hat{R}_q$ belong to the same right coset F_r $(r = 1, \ldots, \sigma)$ of $F_1 \subset O$, the symmetry group of the orientating operator $\hat{F}$, only if there exists an operator $\hat{R}_i \in F_1$ such that

$$\hat{R}_i \hat{R}_p = \hat{R}_q .$$

Applying both sides of this equation to the arbitrary initial orientation v_1, one finds

$$\hat{R}_i \hat{R}_p v_1 = \hat{R}_q v_1 .$$

Taking into account the correspondence between the orientations v_n and the rotations $\hat{R}_n$:

$$v_n = \hat{R}_n v_1 , \tag{A1}$$

one obtains

$$\hat{R}_i v_p = v_q .$$

The rotation of v_p by $\hat{R}_i$ is equivalent to a rotation of $\hat{F}$ by $R_i^{-1} \in F_1$. Because this is a symmetry operation of the orientating operator, $\hat{F}$ is left invariant. Therefore, the population numbers in the two orientations are equal, as stated in Eq. (10b):

$$N_p = N_q .$$

APPENDIX B: PROOFS OF THE RULES GIVEN IN EQS. (12) IN SEC. II B

In the following the transformation of a function $f(T_{ij})$ of the Raman-tensor elements T_{ij} is defined by

$$\hat{R}_p f(T_{ij}) = f((\underline{R}_p \underline{T} \underline{R}_p^t)_{ij}) .$$

If for a general Raman tensor $\underline{T}^{(1)}$ and for $\hat{R}_p \in F_1$:

$$\hat{R}_p (T_{ij}^{(1)} T_{i'j'}^{(1)}) = K T_{st}^{(1)} T_{s't'}^{(1)} , \tag{B1}$$

then this relation also applied to each of the rotated Raman tensors $T^{(n)}$:

$$\hat{R}_p (T_{ij}^{(n)} T_{i'j'}^{(n)}) = K T_{st}^{(n)} T_{s't'}^{(n)} , \tag{B2}$$

because they are also covered by the general tensor $\underline{T}^{(1)}$. From the definition in Eq. 11(b) one derives

$$P_{iji'j'}^{(1)} = \sum_{\hat{R}_q \in F_1} T_{ij}^{(q)} T_{i'j'}^{(q)} = \sum_{\hat{R}_q \in F_1} \hat{R}_q (T_{ij}^{(1)} T_{i'j'}^{(1)}) \ .$$

Taking $\hat{R}_n = \hat{R}_p^{\ -1} \hat{R}_q$, then $\hat{R}_n \in F_1$ and

$$P_{iji'j'}^{(1)} = \sum_{\hat{R}_n \in F_1} \hat{R}_p \hat{R}_n (T_{ij}^{(1)} T_{i'j'}^{(1)})$$

$$= \sum_{v_n \in V_1} \hat{R}_p (T_{ij}^{(n)} T_{i'j'}^{(n)}) \ . \tag{B3}$$

Combining Eqs. (B2) and (B3)

$$P_{iji'j'}^{(1)} = K \sum_{v_n \in V_1} T_{st}^{(n)} T_{s't'}^{(n)} = K P_{sts't'}^{(1)} \ . \tag{B4}$$

The above equation is equivalent with

$$\sum_{\hat{R}_p \in F_1} \hat{R}_p (T_{ij}^{(1)} T_{i'j'}^{(1)}) = K \sum_{\hat{R}_p \in F_1} \hat{R}_p (T_{st}^{(1)} T_{s't'}^{(1)}) \ .$$

If this is valid for an arbitrary symmetrical tensor $\underline{T}^{(1)}$, it also applies to each of the rotated tensors $\underline{T}^{(n)}$:

$$\sum_{\hat{R}_p \in F_1} \hat{R}_p (T_{ij}^{(n)} T_{i'j'}^{(n)}) = K \sum_{\hat{R}_p \in F_1} \hat{R}_p (T_{st}^{(n)} T_{s't'}^{(n)}) \ ,$$

$$\sum_{\hat{R}_p \in F_1} \hat{R}_p \hat{R}_n (T_{ij}^{(1)} T_{i'j'}^{(1)}) = K \sum_{\hat{R}_p \in F_1} \hat{R}_p \hat{R}_n (T_{st}^{(1)} T_{s't'}^{(1)}) \ .$$

If $\hat{R}_n \in F_r$, then the summation over $\hat{R}_p$ turns into a summation over $\hat{R}_q = \hat{R}_p \hat{R}_n$ with $\hat{R}_q \in F_r$:

$$\sum_{\hat{R}_q \in F_r} \hat{R}_q (T_{ij}^{(1)} T_{i'j'}^{(1)}) = K \sum_{\hat{R}_q \in F_r} \hat{R}_q (T_{st}^{(1)} T_{s't'}^{(1)}) \ ,$$

or equivalently, for each coset F_r:

$$P_{iji'j'}^{(r)} = K P_{sts't'}^{(r)} \ ,$$

and for the total IP:

$$P_{iji'j'} = \sum_r \mathscr{N}_r P_{iji'j'}^{(r)} = K \sum_r \mathscr{N}_r P_{sts't'}^{(r)} = K P_{sts't'} \ , \tag{B5}$$

as was quoted in (12b).

Finally the proof leading from Eqs. (12c) to Eq. (12d) is a special case of the proof given above. Taking Eq. (B4) with $K=0$ as the original condition, Eqs. (12c) and (12d) can be proven with the same procedure which leads to conclusion Eq. (B5).

APPENDIX C: PROOF OF EQS. (13) IN SEC. II C

Two rotations $\hat{R}_p$ and $\hat{R}_q$ belong to the same left coset O_r $(r=1, \ldots, \sigma')$ of the defect symmetry group O_1 if and only if there exists an operator $\hat{R}_i \in O_1$ such that

$$\hat{R}_p \hat{R}_i = \hat{R}_q \ .$$

If both sides of this equation are applied to the arbitrary initial orientation v_1 one finds

$$\hat{R}_p \hat{R}_i v_1 = \hat{R}_q v_1 \ . \tag{C1}$$

The initial orientation v_1 is, however, invariant under the operators of the symmetry group O_1 of the defect

$$\hat{R}_i v_1 = v_1 \ . \tag{C2}$$

Combining Eqs. (C1) and (C2) yields

$$\hat{R}_p v_1 = \hat{R}_q v_1 \ ,$$

and by the correspondence between the rotations $\hat{R}_n$ and the orientations v_n [Eqs. (A1)] it is found that

$$v_q = v_p \ ,$$

as was stated in Eq. (13b).

APPENDIX D: INTERNAL SYMMETRY OF THE EQS. (9) (SEE SEC. II D 1)

The set of variables in Eqs. (9) (Sec. II A) is given by

$$X = (T_{11}, T_{22}, T_{33}, T_{23}, T_{13}, T_{12}, M_1, \ldots, M_6, M'_1, \ldots, M'_6, M''_1, \ldots, M''_6, M'''_1, \ldots, M'''_6) \ , \tag{D1}$$

in which we employ the linear combinations M_m, M'_m, M''_m, and M'''_m of the population numbers N_n [see Table III(b)]. Equations (9) are explicitly given in Table III(a). The following three permutations $\hat{P}_{ij}$ of the set of variables (D1) leave Eqs. (9) [Table III(a)] invariant:

$$\hat{P}_{12} X = (T_{22}, T_{11}, T_{33}, T_{13}, T_{23}, T_{12}, M_2, M_1, M_6, M_5, M_4, M_3, M'_2, \ldots, M'''_3) \ ,$$

$$\hat{P}_{13} X = (T_{33}, T_{22}, T_{11}, T_{12}, T_{13}, T_{23}, M_4 M_6, M_5, M_1, M_2, M_3, M'_4, \ldots, M'''_3) \ ,$$

$$\hat{P}_{23} X = (T_{11}, T_{33}, T_{22}, T_{23}, T_{12}, T_{13}, M_3, M_5, M_1, M_6, M_2, M_4, M'_3, \ldots, M'''_4) \ ,$$

in which the sets of M'_m, M''_m, M'''_m permute in the same way as the set of M_m. The indices of the permutations $\hat{P}_{ij}$ indicate the permutations of the indices of the Raman-tensor elements T_{ij}.

Taking into account, on the one hand, the relations between the population numbers M which result from the defect symmetry O_1 (Sec. II C), and, on the other hand, the specific expressions of the Raman tensors (Table V), it is found that, as a result of this permutation symmetry, the modes $D_2[100]:B_1$, B_2, and B_3 cannot be distinguished from each other: One cannot make a distinction between them on the basis of Raman measurements only.

*Permanent address: Physics Department, Beijing University, Beijing, China.

[1]R. Claus, L. Merten, and J. Brandmüller, *Springer Tracts in Modern Physics* (Springer, Berlin, 1975), Vol. 75.

[2]D. A. Long, *Raman Spectroscopy* (McGraw-Hill, New York, 1977).

[3]M. Tinkham, *Group Theory and Quantum Mechanics* (McGraw-Hill, New York, 1964).

[4]J. F. Zhou, E. Goovaerts, and D. Schoemaker, following paper, Phys. Rev. B <u>29</u>, 5533 (1984).